atmosphere

MDPI

Article

Odour Emissions and Dispersion from Digestate Spreading

Maria Raffaella Vuolo [1,*], Marco Acutis [2], Bhishma Tyagi [3], Gabriele Boccasile [4], Alessia Perego [2] and Simone Pelissetti [1]

[1] UptoFarm s.r.l., 10095 Grugliasco, Italy
[2] Department of Agricultural and Environmental Sciences, University of Milan, 20133 Milan, Italy
[3] Department of Earth and Atmospheric Sciences, National Institute of Technology Rourkela, Rourkela 769008, India
[4] Direzione Generale Agricoltura, Alimentazione e Sistemi Verdi, 20124 Milan, Italy
* Correspondence: mariar.vuolo@uptofarm.com

Abstract: Odour emissions from digestate applied on 21 October 2020 in a 2.4 ha field in the Po Valley (Casalino, 28060, Novara, Italy) were measured using dynamic olfactometry and a six-specialist odour panel, and two application techniques were compared. The measured odour emissions were 3024 and 1286 ou m^{-2} h^{-1}, corresponding to the digestate application with surface spreading and direct injection, respectively. The odour dispersion for the different emission values was modeled to a distance of approx. 500 m from the center of the field and 15 m from the ground using a Lagrangian puff model (SCICHEM) in different meteorological conditions. The meteorological variables were measured at the closest station during the whole month in which the digestate application took place, mimicking a "worst-case scenario" characterized by the frequent applications along the considered period. The maximum odour concentrations within one square km area from the center of the field occurred in calm wind and stable atmospheric conditions. This study also evaluated the effect of a barrier downwind from the source. In the worst-case scenario (spreading technique with maximum emissions, no barriers), the average and maximum estimated odour concentrations were 3.2 and 18.9 ou m^{-3}, respectively. The calculated probabilities of exceeding the threshold value of 1 ou m^{-3} were 36% and 47% for the whole period and the episodes of calm winds, respectively, and 14% on average for the episode of maximum wind gust. In the best emission scenario (direct injection), the average and maximum odour concentrations were 1.5 and 8.6 ou m^{-3}, respectively, while the probabilities of exceeding 1 ou m^{-3} were 26% and 36% for the whole period and the episodes of calm winds, respectively, and 0.016% for the maximum wind gust episode. In the presence of a solid barrier downwind from the source and for the wind gust episode, the peak values of the concentrations and exceedance probabilities at the sampling height were found to be reduced by a factor close to 2.5 and 5×10^5, respectively. The study also evaluated the concentration field's vertical distribution, showing that the odour plume's vertical and horizontal dispersion slightly increased with the barrier. This is not a cause of concern unless the emitted substances causing odour nuisance are also atmospheric pollutants with potential harm to far-field ecosystems and human settlements at low concentration levels.

Keywords: SCICHEM model; Lagrangian and puff modeling; digestate incorporation; barrier effect

Citation: Vuolo, M.R.; Acutis, M.; Tyagi, B.; Boccasile, G.; Perego, A.; Pelissetti, S. Odour Emissions and Dispersion from Digestate Spreading. *Atmosphere* **2023**, *14*, 619. https://doi.org/10.3390/atmos14040619

Academic Editors: Martin Piringer, Günther Schauberger and Wenjing Lu

Received: 15 February 2023
Revised: 18 March 2023
Accepted: 20 March 2023
Published: 24 March 2023

1. Introduction

A sensation from inhaling volatile chemicals (e.g., sulfur, nitrogen, and volatile organic compounds) is called an odour [1]. Anthropogenic activities are mainly responsible for odour issues in the environment, including agricultural and industrial activities, wastewater treatment plants, landfills, livestock buildings, petrochemical parks, foundries, slaughterhouses, composting activities, and paper and pulp facilities [2–5]. odours adversely affect health, depreciate property prices, and increase annoyance [6–8]. Recent studies considered

odour as an atmospheric contaminant [9,10]. Odour nuisances are often reported to public authorities in agricultural areas, especially with intense livestock activities.

Odour modeling is a challenging problem from both a scientific and regulatory perspective [11]. Nowadays, odour dispersion is treated with tools similar to those with better characterized atmospheric pollutants. However, some widely accepted assumptions used in air pollution modeling do not hold for odour dispersion [12]. For example, mass conservation is not strictly applicable when assimilating an odour to a transported scalar in a model, and the chemical nature of odourous compounds is seldom known. Additionally, most common atmospheric dispersion models provide mean concentrations at the integration time step, generally 15 min to 1 h, which are much larger than the relevant time scale for odours perception (a few seconds). This problem is mainly related to the intrinsic limitations in the models' abilities to represent the instantaneous features of turbulent atmospheric flows. It is, therefore, not a straightforward task to address. Several approaches rely on empirical estimations of the output concentration probability distribution and assume a particular value for the "peak-to-mean ratio", which can possibly vary in time and space [13,14]. Higher-order closure methods are considered more reliable as they derive the concentration variance by solving equations that describe the physical properties of atmospheric turbulence [15].

In addition, the measurements needed to feed odour dispersion models are also affected by several challenges and uncertainties, thus adding complexity to the problem. From the regulatory point of view, institutions and authorities face the challenge of establishing objective criteria and limitations despite the subjective nature of odour nuisances that are mediated by human perception. Despite the difficulties, several approaches and tools have been developed and are currently used to measure, model, and regulate atmospheric odour dispersion [7,16]. Atmospheric dispersion models are often used as a support for authorization decisions and regulation procedures and in case of litigation due to reported odour nuisances. Their use in agricultural areas is nevertheless mostly limited to the livestock sector. At the same time, odour emissions from manure spreading are seldom measured and modeled without any published dataset on the issue.

The present work focuses on odour dispersion modeling, with input data derived from field measurements over the Po Valley, Italy. Northern Italy, and in particular the Po Valley, is one of the areas with the highest levels of intensive farming and concentrations of biogas plants worldwide [17]. The sole Lombardy region in this area accounts for a large part of the total Italian livestock, in particular more than 27% of cattle and 51% of pigs [18]. We used a Lagrangian puff model for the odour dispersion estimation. The simulations were performed for varied wind intensities and considered the effect of a solid barrier downwind from the source. The paper is structured as follows. Section 2 describes the experimental site and the measurements of both the odours and meteorological variables, Section 3 describes the selected model and the simulation scenarios, and Section 4 presents the results of the simulations.

2. Materials and Methods

2.1. The Experimental Site

The experimental site was located in Casalino (45.34598 N, 8.497738 E), Italy, and the surface of the fertilized field was 2.4 ha. This area was characterized by its intensive agriculture, with significant production and use of organic fertilizers. The orography was smooth and the agricultural fields were often contiguous or at a small distance from human settlements. Figure 1 shows the topographic map of the area, with the measurement site highlighted in blue and red (the different colors correspond to the two tested spreading techniques explained in the Section 2.2). The soil was bare during the fertilization event.

Figure 1. Topographic map of the experimental field, highlighted in red and blue.

2.2. Odour Measurements

The odour emission values used for the simulations were part of a dataset belonging to an experiment whose purpose was to compare the odourous impacts of the different methods of distribution of livestock manure, funded by the EU LIFE PrepAir Project. In this context, three field experiments were carried out in three different locations in northern Italy and in three different periods, where a "local" solution (typically surface distribution followed by incorporation with a harrow) and a "commercial" solution were compared (direct slurry injection via an all-in-one combined spreader (Hydro Tryke by Vervaet, Biervliet, The Netherlands)). For each experimental thesis, five odour emission measurement replicates were carried out for 5–10 min and 4 h after the slurry distribution. The sampling points were chosen using a non-systematic X-shaped sampling (see Figure 2).

Figure 2. Experimental field with the sampling points highlighted in white circles.

The measurements were carried out in accordance with the UNI EN 13725: 2004 standard: "Air quality—determination of odour concentration by dynamic olfactometry", official Italian version of the European Standard EN 13725 (Edition April 2003) [19]. The surveys were carried out using a stainless steel low speed wind tunnel (LSWT) (0.125 m^2 surface covered) through which technical air (grade 5.0) was flown at a flow rate of 30 L/min

for a period of 5 min. At the end of the flushing period, a nalophan bag for the air sampling was connected to the LSWT via Teflon tubing. The sampling was carried out using a vacuum sampler. The samples were subsequently transferred to the analysis laboratory (Osmotech, Pavia, Italy) where the olfactometric analysis was performed within 12 h using the dynamic olfactometer Scentroid SS600 (Scentroid, Stouffville, ON, Canada) and six-specialist odour panel in a binary forced choice mode to determine the odour concentration (ou_e/m^3). Starting with the odour concentration data, the specific odour emission rate (SOER, Ou_e m^2 h) was calculated as a function of the flow intensity and the surface covered by the LSWT. The emission flux measurements took place on 21 October 2020.

Two spreading techniques were tested: direct injection (blue area in Figures 1 and 2) and surface spreading, followed by incorporation (combined disc harrowing of a 10 cm depth) within 12 h (red area in Figures 1 and 2). In the case of the odour emissions measurements at 0 h and 4 h, the harrowing was not relevant since it was performed after the sampling. For the sake of our study, the second technique should, therefore, be intended as "surface spreading". Direct injection is commonly indicated as a technique for mitigating odour and other pollutant emissions, and our measurements confirmed this behavior. The measured emissions in ou (odour units) m^{-2} h^{-1} used in the following as an input for the model are shown in Table 1. The digestate came from the anaerobic digestion of cattle slurry, poultry manure, and energy crops, and details about its chemical composition and application can be found in Appendix A.

Table 1. Odour emission measurements at the moment of digestate application (t1) and after 4 h (t2) for the two studied application techniques.

Treatment	SOER (ou m^{-2} h^{-1})	
	t1 = 0 h	t2 = 4 h
Surface spreading	3024.0	2611.2
Direct injection	1373.0	1262.0

The values shown in Table 1 were in line with previously measured emissions in the Po Valley [5,17]. Considering that a reduction in the emissions was observed after 4 h from the application, we kept the first measurement for the simulations and used it as a constant value throughout the month during which the application took place. This model configuration represented a "worst-case" but still realistic scenario (corresponding to frequent applications on different fields of the same region, during the whole month of October 2020). Therefore, only the data from the column t1 = 0 h of Table 1 were used in our simulations.

2.3. Meteorological Measurements

To model the typical odour emission–dispersion scenarios in the studied region, the simulations were carried out using hourly meteorological data (temperature, wind, humidity, and precipitation) for the whole month of October 2020, during which the slurry application took place. These data were measured at the station "Casello Ruggerina" (Vercelli), 8 km from the experimental site. The meteorological measurements were routinely carried out by Arpa Piemonte—Dipartimento Sistemi Previsionali on a network of stations in the Piemonte region, and they are made available upon request.

Figure 3 shows the time series of the most relevant measured variables for the dispersion model (air temperature, wind speed, and direction), together with the turbulence parameters u* and L derived from the measurements by using the meteorological routines of SCICHEM. Figure 4 shows the average diurnal cycles of the abovementioned variables throughout the month of October 2020. The wind rose in Figure 5a shows that wind most frequently blows from North/Northwest, but the strongest winds most frequently blow from Southeast/East. The wind rose diagram in Figure 5b was drawn using the dataset of the gust events (maximum value recorded by the anemometer in a one-hour interval)

and shows a remarkable prevalence of strong wind events from the East/Southeast. In particular, the maximum wind gust event occurred on 3 October 2020, at 2 a.m., with a wind speed value of 13.6 m s^{-1} and a wind direction of 101 deg from the North. Considering that the odour plume is susceptible to reaching longer distances in stable conditions with moderate to intense wind speeds, we analyzed a nocturnal, statically stable wind gust event and evaluated, in this case, the mitigation potential of a barrier, employing the building downwash algorithm implemented in SCICHEM.

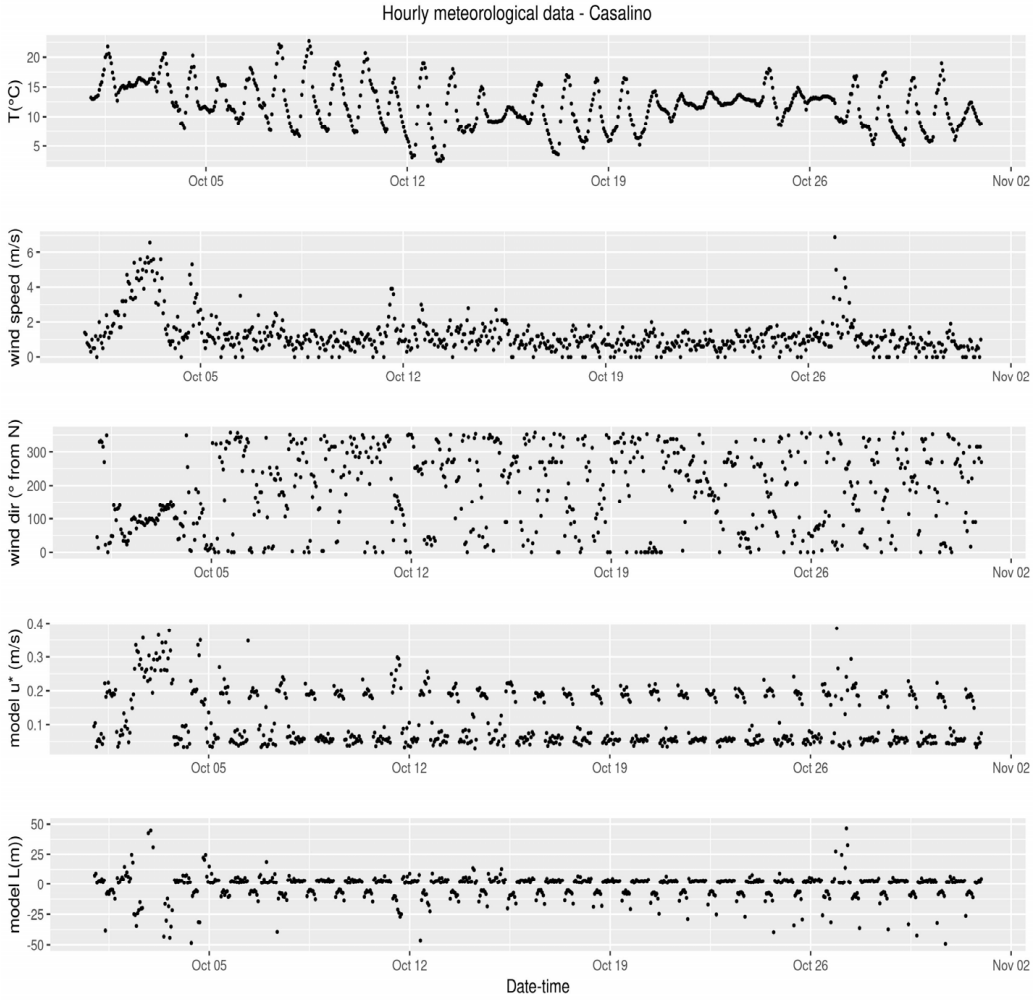

Figure 3. Time series of hourly air temperatures, wind speeds, and directions measured at the closest meteorological station, together with the model-derived values of u* and L. Data refer to the period 1 October 2020–31 October 2020.

On the other hand, "calm winds" conditions are also relevant for pollutant and odour dispersion. Indeed, in these conditions, the dilution effects of the winds and turbulence are reduced, and the pollutants can accumulate near the source regions. The upper threshold for the "calm winds" detection was chosen according to the requirements of the Italian regulation [20], as the value of the wind for which the model applies a dedicated algorithm for dispersion calculations. The rationale for this choice was that these algorithms are generally less accurate than those used in "normal wind" conditions and could, therefore, affect the final estimation of the odour concentrations and exceedance probabilities. The threshold was chosen to be 0.6 m s^{-1} as this corresponded to the "calm winds" flag in SCICHEM. According to this definition, 19% of the records during the month of the simulation fell in the category of "calm winds". Table 2 summarizes the main statistics of the principal variables used by the model in our simulations. The values were in line with the typical meteorological conditions of the region and the considered season.

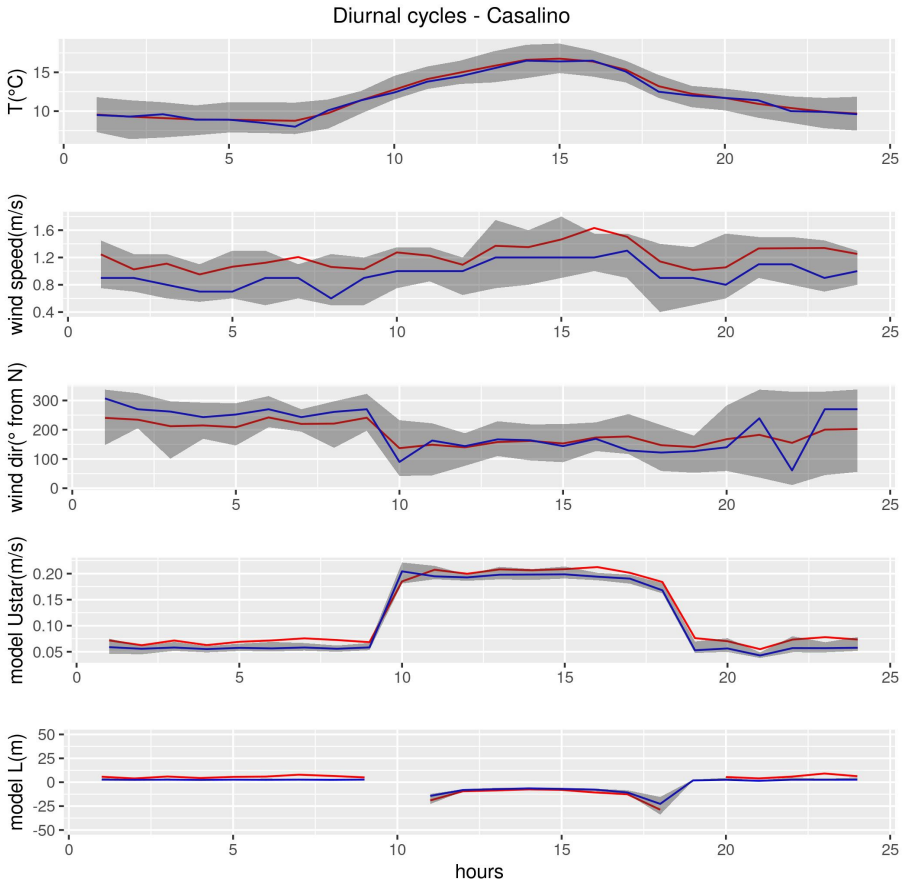

Figure 4. Diurnal cycle of measured air temperatures, wind speeds, and directions, together with the model-derived values of u* and L. Data refer to the period 1 October 2020–31 October 2020. Red/blue lines represent the mean (median) values, and the shaded areas the interquartile ranges (25% and 75%).

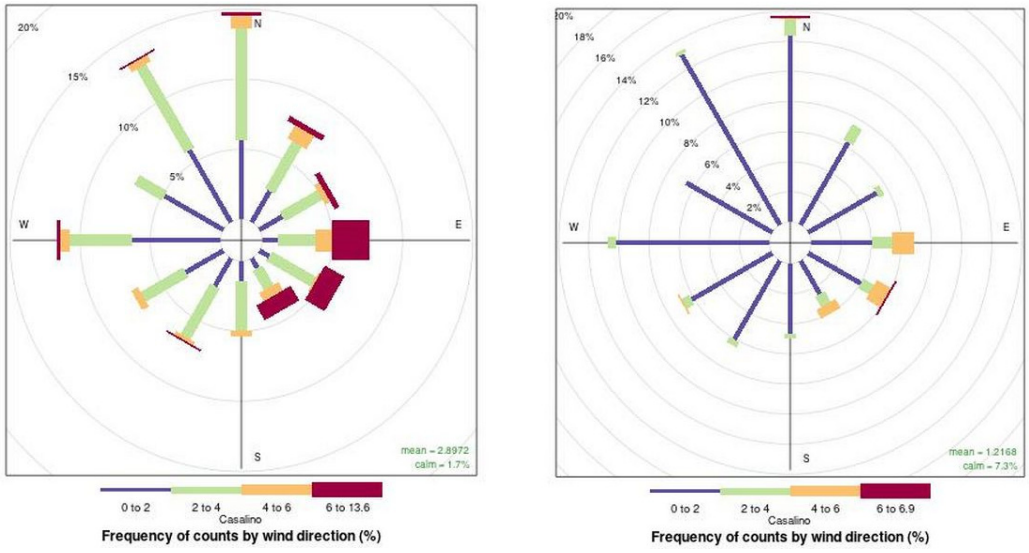

(**a**) (**b**)

Figure 5. Wind rose of hourly mean values (**a**) and gust (**b**) for the period 1 October 2020–31 October 2020. Spoke's length represents the frequency of the wind blowing from the identified direction, while the color(s) within the spoke indicate the percentage of counts with the wind speeds for a certain interval.

Table 2. Main statistics of the meteorological variables used in the present simulations: minimum, 1st and 3d quartiles, median, mean, and maximum.

Statistics	Temperature (°C)	Wind Direction (° from N)	Wind Speed (m s^{-1})	Wind Gust (m s^{-1})
Min.	2.5	0	0	0.8
1st Qu.	9.2	81.5	0.7	1.8
Median	11.9	205	1	2.4
Mean	11.91	186.7	1.238	2.921
3rd Qu.	14.5	288	1.4	3.1
Max.	22.7	357	6.9	13.6

2.4. Odour Dispersion Modeling

2.4.1. The Selected SCICHEM Model

The atmospheric dispersion model suitable for odour modeling was selected based on the requirements and preference criteria listed below.

- In line with the Italian regulations, particularly that of the Lombardy Region that commissioned the study [20].
- In line with the standard UNI 10796:2000 that specified the classes of the models that are recommended as applicable to the problem of odour nuisances (i.e., non-stationary puff models/segment models, 3D Lagrangian puff or particle models, 3D Eulerian models).
- Spatial and temporal scales compatible with the problem under analysis.
- Transport and turbulent schemes adequately representing the peculiarities of odour dispersion.

The preference criteria for selecting SCICHEM were as follows.

- Able to represent the aerodynamic effect and mitigation potential of the barriers.
- Able to represent the inhomogeneous surfaces and the effects of canopies.
- Actively used and maintained by the scientific community, multi-platform and open source.
- User friendly and with low–moderate computational resources requirements for easy use in non-academic contexts (e.g., administrative/regulatory).

SCICHEM, which stands for SCIPUFF (Second-order Closure Integrated Puff) with CHEMistry [21–24] was selected after reviewing more than 50 models with similar purposes [7,25,26] and several methodological guidelines that often contained the models' categorization and reviews [27–29]. More details about the selection criteria and the analyzed models are provided in Appendix B.

SCICHEM, SCIPUFF, and other Lagrangian puff dispersion models calculate the pollutant concentration from the superposition of three-dimensional puffs, which can be viewed as packages of material released from the source, advected by the mean wind, and dispersed according to the turbulence. The representation of the dispersion can be analogous to that of classic Gaussian plume models, with more or less empirical parametrizations of the dispersion coefficients. At the same time, advection (advance in the puff centroid) is coupled with a puff splitting/merging scheme that ensures adequate resolution and mass conservation. The governing equations of the SCICHEM model were widely documented [22,30,31]. Therefore, the present work only highlights the main features of the SCICHEM model that are particularly suitable for odour modeling (i.e., flexibility in meteorological input requirements and second-order closure scheme for turbulence).

Concerning the meteorology, SCICHEM is very flexible in the required input, since it embeds a series of meteorological routines that estimate/calculate all the necessary boundary layer variables when they are not provided in input. The minimum requirement is a single wind vector, but when available, the model can consider observations from a network of sensors measuring the turbulence characteristics, boundary layer height,

and other variables in the form of vertical profiles or gridded data typically provided by meteorological models or pre-processors. Additionally, SCICHEM can use the specified topography to interpolate the measured fields and ensure mass conservation. Our case is somehow intermediate, and the meteorological variables at our disposal consisted of the following.

1. Mean wind (intensity and direction)
2. Wind gust (intensity and direction)
3. Air temperature

All the variables above were provided as hourly means from a measurement height of 10 m for the wind variables and 2 m for the temperature. The air temperature used in the boundary layer calculations of the model should be representative of the surface layer mean temperature. Without additional measurements, we considered that the measurement at 2 m was adequate for the purpose of this study. The stability parameters, such as the friction velocity u* and the Monin–Obukhov length L, are estimated from the input variables (considering also the geographical location, date, and time of the day for the estimation of radiation), with an iterative technique that started from a "first guess" value for L. An iterative scheme is needed since L depends on u* and u* on L [32]. Details on this methodology are explained in the technical documentation [33], in particular the section 10.1.1 "Monin–Obukhov Length, L" and 10.1.2 "Friction Velocity, u*". The parameters L and u* that were derived in this way for our simulations are reported together with the measured meteorological variables in Figures 3 and 4.

The atmospheric turbulent dispersion in SCICHEM is modeled using a second-order closure scheme, which allows for simulating the variance of the concentration field. This renders SCICHEM particularly suitable for modeling odours and other substances where the short time fluctuations are equally or more relevant than the average values of highly toxic, flammable, and explosive materials [34].

The main equations governing the puff dynamics can be derived from the conservation principles and can be expressed in terms of the first and second spatial moments of the concentration.

$$\frac{d\overline{x}_i}{dt} = \overline{u}_i(\overline{x}) + \frac{\left\langle \overline{u_i' c'} \right\rangle}{Q} \tag{1}$$

where x_i are the coordinates of the puff centroid, ui represents the local atmospheric velocity field, and Q is the total mass (integrated concentration of the puff).

The second-moment equation can be obtained by multiplying Equation (1) by $x'i\ x'j$, with $x'i = xi - <x>\ i$, and integrating it in parts

$$\frac{d\sigma_{ij}}{dt} = \sigma_{ik}\frac{\partial \overline{u}_j}{\partial x_k} + \sigma_{jk}\frac{\partial \overline{u}_i}{\partial x_k} + \frac{\left\langle x_i' \overline{u_j' c'} \right\rangle}{Q} + \frac{\left\langle x_j' \overline{u_i' c'} \right\rangle}{Q} \tag{2}$$

where x_i are the coordinates of the puff centroid and σ_{ij} is the matrix of the second moments that describe the spatial dispersion and distortion of the puff. As can be seen from Equations (1) and (2), the third-order moments appear in the equations for the first- and second-order moments. This is the typical "turbulence closure problem" introduced by Reynolds that averages the conservation equations and is addressed in SCIPUFF/SCICHEM by parametrizing the third-order moments as in [35]. This allows the system of equations to be closed.

The final concentration at each point is calculated as a superposition of the contributions from all the puffs in that point, eventually considering the following contributions: the reflections at the top and bottom boundaries, chemical reactions, deposition, and background species concentrations. The concentration variance is also provided in the output using the second-moment equation. The model then obtains the probability distribution by assuming a clipped or truncated Gaussian shape that is obtained from the Gaussian normal distribution by replacing the non-physical negative values with zero values. The

atmospheric observations show that this distribution is the most suitable to describe the short-term atmospheric fluctuations [36,37].

Another aspect that made SCICHEM particularly suitable for our purposes was the great flexibility in the input data requirements. The model can be run either with a minimal set of simple meteorological data, most likely for routine monitoring/regulatory purposes, but also with complex measurements derived from state-of-the-art measurement and modeling techniques (mostly for research purposes).

In addition, SCICHEM can be used from the local (<1 km) to the continental scale and it allows for the simultaneous activation of multiple sources, chemistry simulations, dry and wet deposition, and can account for the effect of the barriers using the PRIME (plume rise and building downwash) scheme [38].

The PRIME algorithm allows for the evaluation of the potential impact of solid obstacles on the pollutant concentrations, simulating the aerodynamic perturbations of the wind and turbulence fields. The barrier induces multiple disturbances on the wind and turbulence fields. First, it decreases the horizontal wind speed at low heights, both upwind and downwind, while it deflects the wind streamlines by adding a vertical component to the wind on the windward side and a negative component on the leeward side (plume rise and downwash effects). An increase in the turbulent kinetic energy comes along with the reduction in the mean wind as a result of large atmospheric eddies being broken into smaller eddies by the obstacle (see [39] and references therein).

The development of the tool was initially motivated by the search for criteria to establish minimum stack heights in urban and industrial contexts. Therefore, it was designed for point sources. At present, the models implementing PRIME (AERMOD, ISC, SCIPUFF/SCICHEM) do not allow for simulations with barriers/buildings in the presence of the area or volume sources. For this reason, when evaluating the effects of the barrier on odour dispersion, the field source was replaced by a point source of a large diameter (40 m). SCICHEM can indeed attribute a finite diameter to point/stack sources and specify their height (0 in our case). We used the same total emission as the one measured from the field in the "best-case scenario" to mimic the combined effect of the injection and the presence of the barrier to mitigate the dispersion.

To our knowledge, this is the first application of the SCICHEM model in the framework of odour dispersion.

2.4.2. Selected Simulation Scenarios

Four different scenarios were simulated, and for each of these, different wind and stability conditions were analyzed. The simulation scenarios referred to the different fertilizer application techniques (thus different emission values) and the eventual presence of a barrier. Table 3 summarizes the characteristics of each scenario: the application technique, emission intensity, and eventual presence of a barrier. As already mentioned, the presence of a barrier could only be simulated in SCICHEM using point sources. Therefore, in addition to the "real scenarios" (1 and 2), two hypothetical scenarios (2bis and 2bis0) were simulated, where the source was replaced by one type "point" with a relatively large diameter (40 m) and the same total emission as scenario 2. In this way, we tested the mitigation potential of the combined effect of direct injection (reduced emissions with respect to scenario 1) and the barrier. Using a very large diameter with a point source posed numerical problems. Therefore, the total area of the source was smaller than the real field.

SCICHEM is also very flexible in the output format, which can be provided at a maximum of 500 receptors and whose location can be specified by the user. In our simulations, the odour concentrations were simulated for a grid of 484 receptors uniformly distributed on a 1 km $\times$ 1 km region centered on the fertilized field for scenarios 1 and 2, and a 200 m $\times$ 200 m region for scenarios 2bis0 and 2bis. Additionally, vertical slices of the concentrations were simulated by placing the 484 model receptors along a transect crossing the fertilized field in the East–West direction, passing by the field's center and reaching a 15 m height. In the horizontal field simulations, the receptors were placed at a 1.7 m

height, representative of human perception. The exceedance probabilities of the threshold value of 1 ou m^{-3} were also calculated for the same horizontal and vertical networks of the model receptors. The value of 1 ou m^{-3} is the lowest among the three thresholds identified by the regional regulation on odour monitoring: 1, 3, and 5 ou m^{-3}, corresponding to the concentrations at which 50%, 85%, and 90–95% of the population perceive the odour sensation [20]. The choice of the lowest threshold represented a "worst case scenario" in terms of the exceedance probabilities.

Acknowledging the limitations of representing a field with a point source in the model, we adopted the following measures to mimic the real scenario as closely as possible.

- The diameter of the point source was set as large as possible (40 m diameter, about 0.1 ha), compatibly with numerical stability.
- The height of the point source was set to zero.
- The ejection velocity and buoyancy effects, typical of a point/stack source, were set to zero as the field was a passive source.
- The total emission value was set equal to that of scenario 2.
- The meteorological data were those of the wind gust event occurring in scenario 2.

The choice of the nocturnal wind gust event was motivated by the fact that, in these conditions, the pollutant/odour plume is susceptible to reach larger distances and the barrier to affect the plume transport and dispersion to a greater extent.

The other relevant configuration parameters (common across all the scenarios) were as follows.

- The fertilized field shape (Figures 1 and 2) was approximated by a square of the same area as that of the experimental field.
- The mass effects (inertia, gravity) of the transported quantity were not considered.
- The chemical reactions were not considered.
- The deposition was switched off.
- The surface roughness length was set to 0.01 m (rough, bare soil).
- The maximum number of receptors allowed by the model is 500, therefore, we set a grid of 22 × 22 equally spaced receptors across the domain.
- The output time step was set to 15 min.

For scenarios 2bis0 and 2bis, where the field was replaced by a circle source of 40 m diameter, the total domain was reduced to 200 × 200 m, zoomed around the source. For these scenarios, vertical profiles were also simulated. Therefore, in this case, a vertical grid was defined from the ground up to a 15 m height at a constant latitude corresponding to the center of the circular source. For the vertical slices, 22 points were used on the x-axis and 22 vertically to get a good resolution of the zoomed region.

Table 3. Description of the simulation scenarios.

Scenario Name	Fertilizer Application Technique	Emissions	Notes
Scenario 1	Surface spreading	Per unit surface: 3024 ou m^{-2} h^{-1} Total: 2×10^4 ou s^{-1}	Area source
Scenario 2	Direct injection	Per unit surface: 1286 ou m^{-2} h^{-1} Total: 8.5×10^3 ou s^{-1}	Area source
Scenario 2bis0	As Scenario 2	As Scenario 2	Area source replaced by a "point" (stack type) source of 40 m diameter and zero height
Scenario 2bis	As Scenario 2	As Scenario 2	As Scenario 2bis0 + barrier

3. Results

3.1. Modeled Odour Concentration Plume

To analyze an event of potential odour nuisance reaching significant distances from the source, we chose the date and time (3 October 2020 at 2 a.m.) when the maximum wind gust speed was registered (see Section 2.3. Meteorological Measurements).

The simulation domain extent was chosen considering that concentrations larger than 1 ou m^{-3} were observed up to approx. 500 m from the center of the source field (Figure 6). On average over the whole period, the choice of this domain size led to a boundary/peak concentration ratio of 5%. For the 2bis0 and 2bis scenarios, the domain was reduced accordingly, considering that the source extent was smaller in this case.

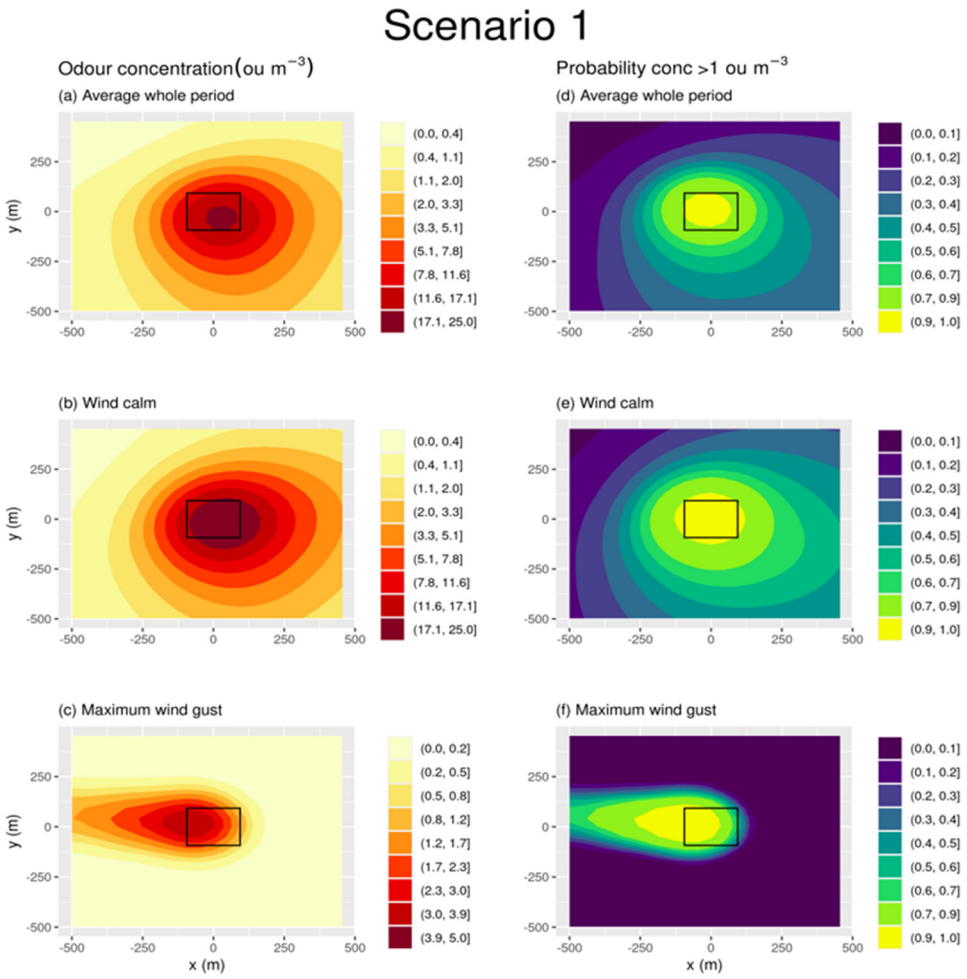

Figure 6. Odour concentrations (left panel) and exceedance probability of the 1 ou m^{-3} threshold (right panel) at a 1.7 m height as simulated by SCICHEM for the period 1 October 2020–31 October 2020, for scenario 1. Modeled concentrations and probabilities are represented for the whole period (**a**,**d**), the episodes of calm winds (**b**,**e**), and the episodes of maximum wind gust (**c**,**f**). The square in the center represents the fertilized field (emission source), and the x and y coordinates are expressed as the distances in meters from the center of the source. Note: the color scale for the concentrations is different in the maximum wind gust event from the other two cases (average conditions, wind calm conditions).

Figure 6 shows that the maximum concentrations along the whole period (a), for the case study of 3 October 2020, at 2 a.m. (b), and during the episodes of calm winds (c) were observed in correspondence with the source and over a roughly elliptical area oriented towards the direction of the prevailing winds (see Figure 5). Averaging only the calm winds episodes, the maximum concentrations increased by a factor of 1.5 due to

accumulation near the source. The whole period concentrations and the concentrations during the calm winds decreased by a factor of 0.2 at approx. 500 m distance from the source. The above-threshold values (>1 ou m^{-3}) were also observed at these distances due to the large emission area and the high value of emissions in this scenario. As for the concentrations observed during the episode of a maximum wind gust, these were generally lower (see Figure 6a,c), likely due to the increased dilution by the transport and turbulence. However, the reduction in the concentration values with the distance was much less than for the calm or average winds. The downwind concentrations at the domain border were still above 1 ou m^{-3}, a value that was only reduced from the peak value at the center of the field by a factor of 0.7. These differences were reflected in the probabilities of exceeding the chosen threshold (1 ou m^{-3}). The mean decreased to approx. 0/0.4 close to the borders of the simulation domain. The gust episode remained close to one and 500 m downwind from the source (Figure 6d–f).

The vertical slices of the concentrations and exceedance probabilities are shown in Figure 7 for the same meteorological cases shown in the horizontal maps. The maximum concentrations (up to 25 ou m^{-3}) were observed for larger heights (up to 2.5 m) in the case of the calm winds compared to both the average period and the wind gust event. The effects of accumulation near the source is visible in Figure 7 and is related to the reduced advection in these meteorological conditions. The shape of the plume was strongly modified by the wind gust, as already observed in the horizontal section, with more pronounced vertical gradients and decreased horizontal gradients in the direction of advection.

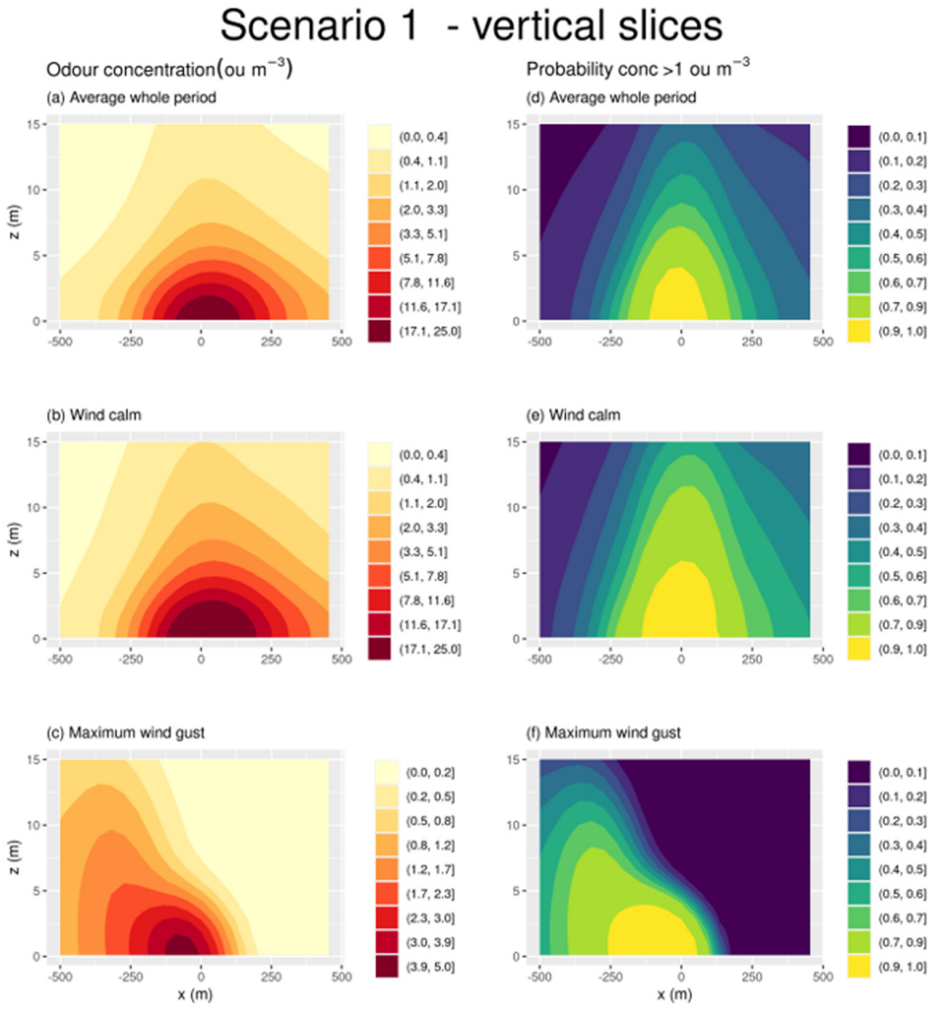

Figure 7. Vertical slices of the odour concentrations (left panel) and exceedance probability of the 1 ou m^{-3} threshold (right panel) for an East–West transect placed at the latitude of the source's center,

simulated by SCICHEM for the period 1 October 2020–31 October 2020, for scenario 1. Modeled concentrations and probabilities are represented for the whole period (**a**,**d**), the episodes of calm winds (**b**,**e**), and the episode of maximum wind gust (**c**,**f**). Note: the color scale for the concentrations is different in the maximum wind gust event from the other two cases (average conditions, wind calm conditions).

3.2. Effect of Stability

Figures 8 and 9 show the SCICHEM results for scenario 1, disaggregated by the stability conditions. The disaggregation was achieved by filtering the output fields on the basis of the model-calculated Monin–Obukhov length L, shown in Figures 3 and 4. Considering the limited amount of input data and the approximations made in the model in order to calculate L, we only differentiated between the stable (L > 0) and unstable (L < 0) cases without going into finer disaggregation (e.g., according to Pasquill stability classes). Both figures show the highly relevant impact of the stability on the concentration fields, with strong dilution effects induced by the daytime convective turbulence. The horizontal maps (Figure 8) show that, at the selected receptors' height (1.7 m), the maximum concentration was reduced by approx. one order of magnitude in the unstable conditions. Figure 9 shows that the plume was more diluted, with lower vertical gradients in the unstable cases, indicating the effect of the increased vertical dispersion.

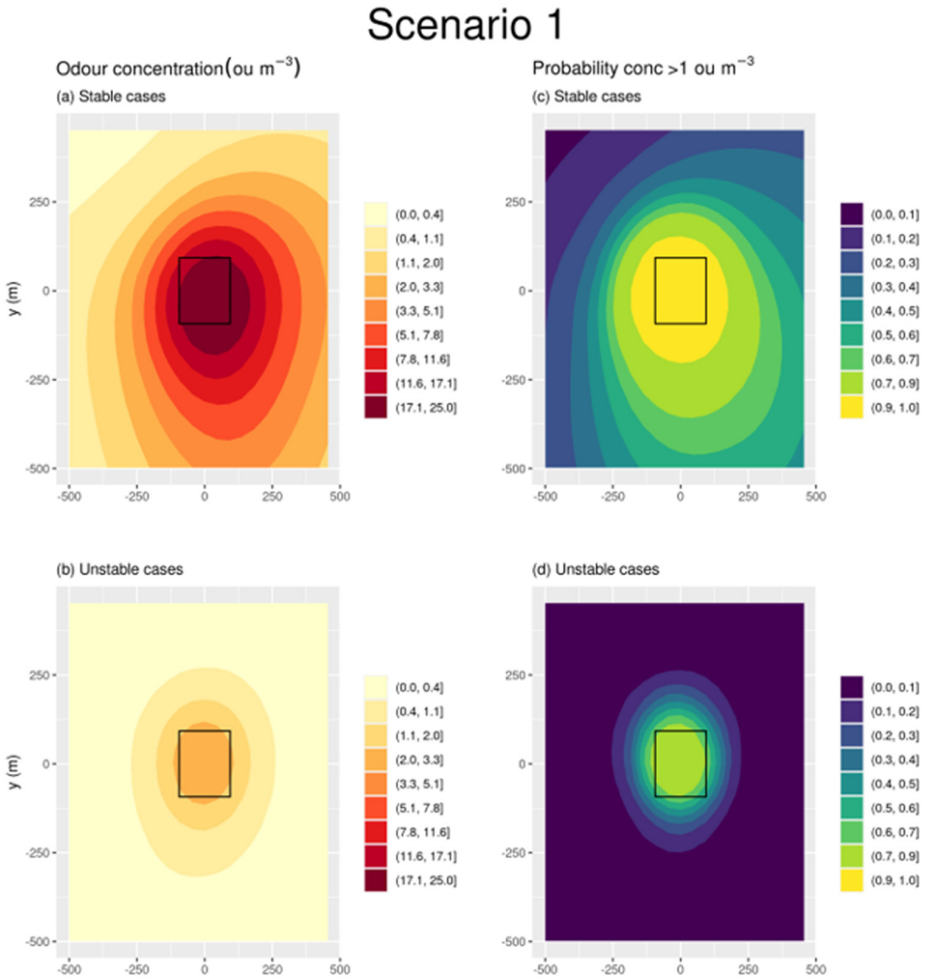

Figure 8. Odour concentrations (left panel) and exceedance probability of the 1 ou m^{-3} threshold (right panel) at a 1.7 m height as simulated by SCICHEM for the period 1 October 2020–31 October 2020, for scenario 1. Modeled concentrations and probabilities are represented for the stable (**a**,**c**), and unstable cases (**b**,**d**). The square in the center represents the fertilized field (emission source), and the x and y coordinates are expressed as the distances in meters from the center of the source.

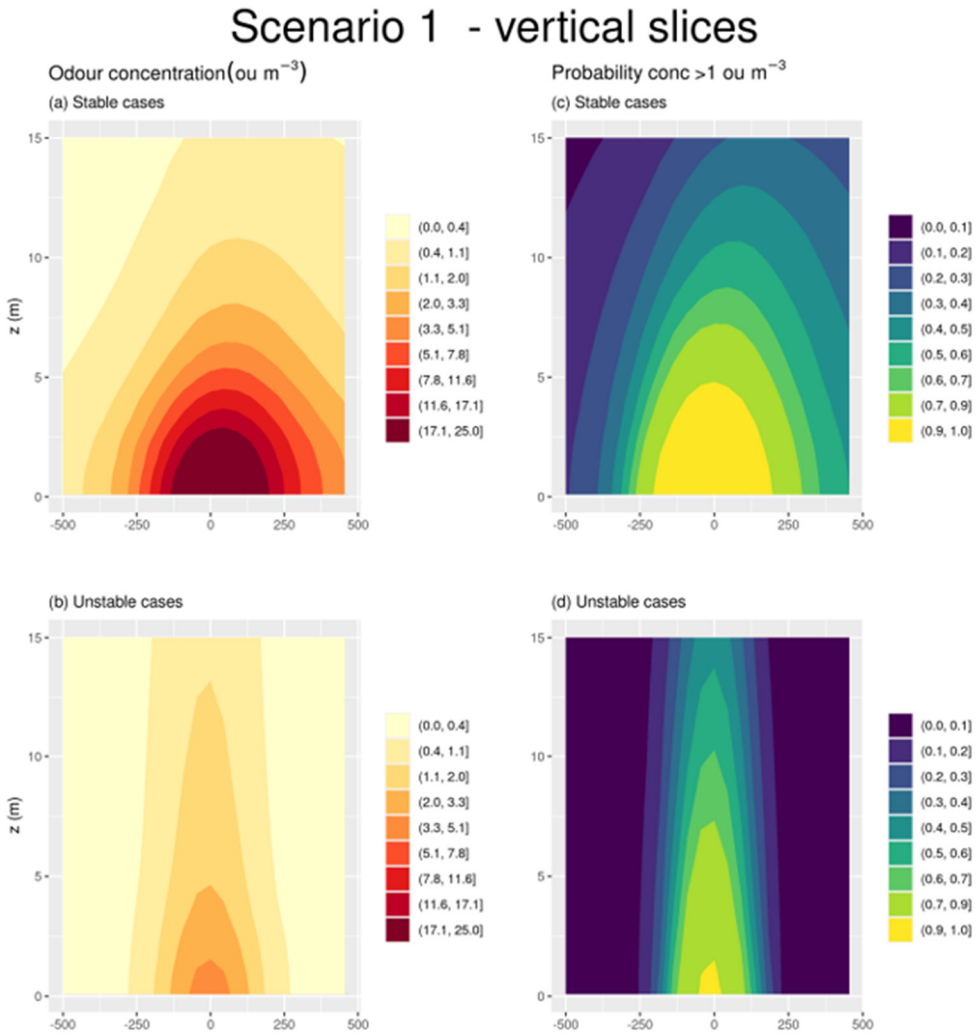

Figure 9. Vertical slices of the odour concentrations (left panel) and exceedance probability of the 1 ou m^{-3} threshold (right panel) for an East–West transect placed at the latitude of the source's center, as simulated by SCICHEM for the period 1 October 2020–31 October 2020, for scenario 1. Modeled concentrations and probabilities are represented for the stable (**a**,**c**), and unstable cases (**b**,**d**). The square in the center represents the fertilized field (emission source), and the x and y coordinates are expressed as the distances in meters from the center of the source.

3.3. Effect of Reduced Emissions

Figure 10 corresponds to scenario 2 with lower emissions and shows the same patterns as Figure 6, with decreased (roughly halved) concentrations in all the meteorological conditions. The exceedance probabilities were also reduced on average by factors of 1.4 and 1.3 for calm winds and 2 and 3 for the wind gust episodes. Notably, the relationship between the exceedance probability and the concentration isnon-linear and strongly depended on the selected threshold. Table 4 summarizes the main statistics of both the concentrations and exceedance probabilities over the whole domain for both scenarios and under the considered meteorological conditions (average, calm, wind gust).

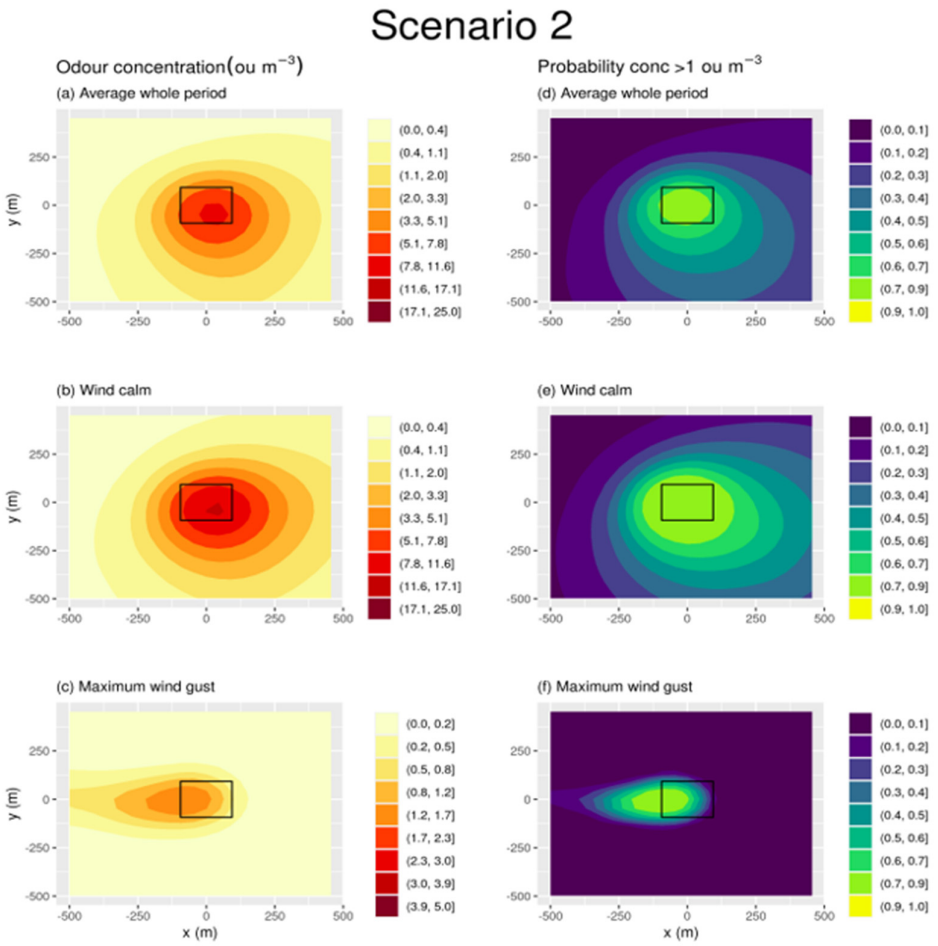

Figure 10. Odour concentrations (left panel) and exceedance probability of the 1 ou m^{-3} threshold (right panel) at a 1.7 m height as simulated by SCICHEM for the period 1 October 2020–31 October 2020, for scenario 2. Modeled concentrations and probabilities are represented for the whole period (**a**,**d**), the episodes of calm winds (**b**,**e**), and the episode of maximum wind gust (**c**,**f**). The square in the center represents the fertilized field (emission source), and the x and y coordinates are expressed as the distances in meters from the center of the source. Note: the color scales are the same as for scenario 1, with those for the concentrations in the maximum wind gust event being different from the other two cases (average conditions, wind calm conditions).

3.4. Effect of Barriers

As explained above, the PRIME model embedded in SCICHEM and in other dispersion models does not simulate barriers for area or volume sources. For this reason, the emitting area of the fertilized field was replaced by a source of type "point" but with a finite diameter. The use of a very large diameter that would allow for the representation of the same area as the real field nevertheless posed some numerical problems. Therefore, the area of the source was reduced to a diameter of 40 m but maintained the same total emission value of scenario 2.

This replacement allowed for the activation of the PRIME module in SCICHEM and, therefore, the quantification of the effect of a barrier by comparison of concentration fields with and without it, for the hypothetical circular source (scenarios 2bis0 and 2bis as defined in Table 3). The effect of the barrier was studied only in the event of the wind gust and placed 1 m downwind from the western edge of the field, which was normal to the incident wind direction. The barrier width (along-wind), length (across-wind), and heights were 1, 40, and 10 m, respectively. The emissions were those corresponding to the application technique that already significantly reduced the emissions and, consequently, the dispersion of odours. In this way, the combined abatement potential of the application technique and the presence of a barrier was evaluated.

Table 4. Odour concentration and exceedance probability statistics for scenarios 1 and 2: minimum, median, mean, 1st and 3d quartiles, maximum. The statistics are provided for the whole period, for the wind calm conditions, and for the wind gust episode.

	Concentration [ou m^{-3}]			Exceedance Probability [-]		
	Whole Period	**Calm Winds**	**Wind Gust**	**Whole Period**	**Calm Winds**	**Wind Gust**
			Scenario 1			
Min.	0.12	0.14	0	0.04	0.07	0
1st Qu.	0.79	1.08	4×10^{-5}	0.19	0.31	0
Median	1.90	2.50	0.01	0.33	0.46	0
Mean	3.23	4.48	0.37	0.36	0.47	0.14
3rd Qu.	3.85	5.33	0.27	0.46	0.61	0.03
Max.	18.86	26.80	3.90	0.96	0.98	0.98
			Scenario 2			
Min.	0.05	0.06	0	0.02	0.02	0
1st Qu.	0.33	0.44	1.93×10^{-5}	0.11	0.17	0
Median	0.83	1.13	2.5×10^{-3}	0.24	0.34	0
Mean	1.46	2.01	0.17	0.26	0.36	0.06
3rd Qu.	1.76	2.38	0.12	0.37	0.5	3×10^{-7}
Max.	8.55	12.03	1.66	0.81	0.88	0.84

The choice of the nocturnal wind gust event was motivated by the fact that during stable and high wind speed conditions the pollutants/odour plume is susceptible to reach the greatest distances, as demonstrated in Figures 6 and 10 (compare panel d with a,b). Additionally, in this condition, and for a barrier placed perpendicularly to the wind direction, its effect was expected to be maximum. As shown in Figures 11 and 12, placing a barrier downwind of the source and perpendicular to the wind direction reduced the maximum odour concentrations approximately by a factor of 2.5. The exceedance probability close to the source was more drastically reduced by five orders of magnitude in its maximum value and became essentially zero on average (Figures 11 and 12, and Table 5). The very large difference between the exceedance probabilities with and without a barrier rendered the exceedance probabilities indistinguishable from 0 in Figure 12 (a common color scale was used between Figures 11 and 12 for both the concentrations and exceedance probabilities).

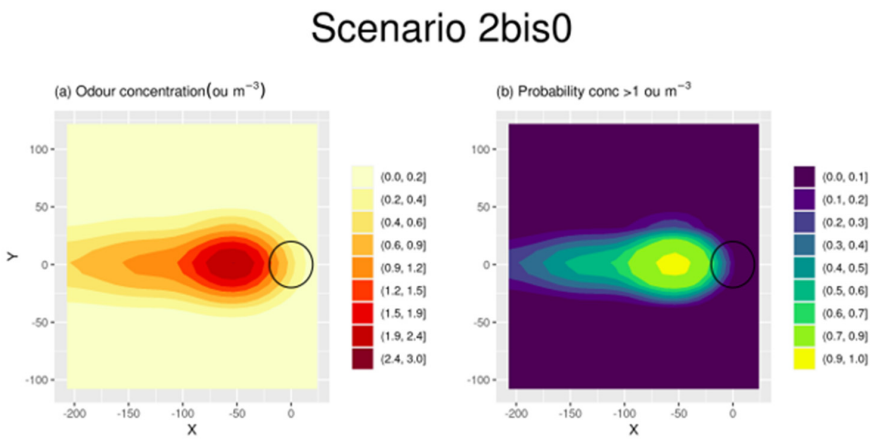

Figure 11. Odour concentrations (**a**) and exceedance probability of the 1 ou m^{-3} threshold (**b**) at a 1.7 m height as simulated by SCICHEM. Meteorology and total emissions are the same as in the wind gust episode of scenario 2, but with the emission field replaced by a 40 m−diameter circular source, represented in black in the graphs. Coordinates x and y are expressed as the distances in meters from the center of the source.

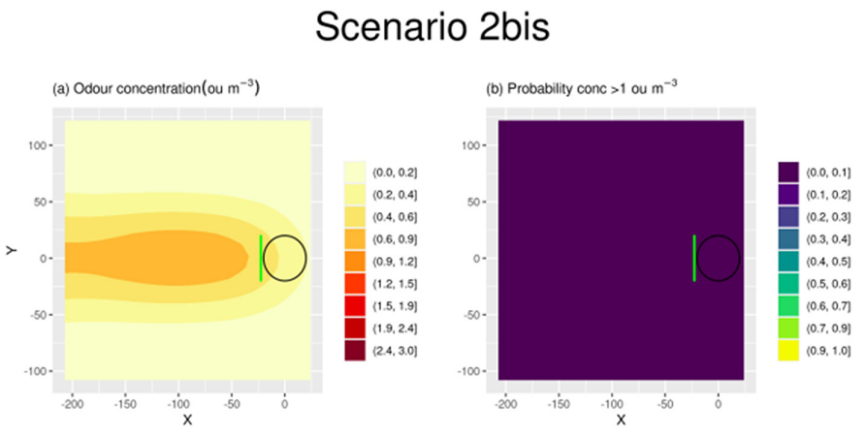

Figure 12. Odour concentrations (**a**) and exceedance probability of the 1 ou m^{-3} threshold (**b**) at a 1.7 m height as simulated by SCICHEM. Meteorology and total emissions are the same as in the wind gust episode of scenario 2, but with the emission field replaced by a 40 m−diameter circular source, represented in black in the graphs. Coordinates x and y are expressed as distances in meters from the center of the source. The barrier is represented as a green rectangle.

These results highlighted the high potential of using barriers to reduce the odour nuisance at the considered height (1.7 m, representative of the human sampling height) in the vicinity of the source, especially if combining them with techniques that favor the capture or deposition of the pollutants upwind or within the barrier itself. Several factors influence the effect of the barrier, including its physical features, location, orientation with respect to the wind, and the physicochemical properties of its material.

The plume appeared slightly more dispersed horizontally in the scenario 2bis (with a barrier), and this was reflected by the statistics of the concentration all over the domain (Table 5). Despite the maximum concentration values being drastically reduced with the barrier, the mean values were slightly higher in this scenario.

Table 5. Odour concentration and exceedance probability statistics for scenarios 2bis0 and 2bis: minimum, median, mean, 1st and 3d quartiles, maximum. Scenarios 2bis0 and 2bis are simulated for the wind gust episode only.

	Scenario 2bis0		**Scenario 2bis**	
	Concentration [ou m^{-3}]	**Exceedance Probability [-]**	**Concentration [ou m^{-3}]**	**Exceedance Probability [-]**
Min.	0	0	2.3×10^{-4}	0
1st Qu.	2.99×10^{-5}	0	0.01	0
Median	7.1×10^{-3}	0	0.09	0
Mean	0.13	0.03	0.15	6.79×10^{-9}
3rd Qu.	0.18	4.9×10^{-5}	0.28	0
Max.	1.20	0.67	0.50	1.26×10^{-6}

Our results show a significant decrease in both the concentration and exceedance probability at the sampling height with the barrier. Nevertheless, considering that the deposition was switched off in our simulations, these results were likely related to a different spreading of the odour in the atmosphere, as also suggested by the statistics across the simulation domain (Table 5). To investigate the fate of the simulated odour, we performed additional simulations by placing the receptors on a vertical slice parallel to the x-axis (along-wind direction for the wind gust event). The slice crossed the simulation domain of scenarios 2bis0 and 2bis at the location of the source center and reached 15 m in height. The results are shown in Figures 13 and 14. These figures confirmed the overall reduction in the concentrations in the vicinity of the source but also highlighted the higher

level of the horizontal and especially vertical dispersion induced by the barrier. Similar to the horizontal graphs, the very large difference between the exceedance probabilities with and without a barrier rendered the exceedance probabilities indistinguishable from zero in Figure 14 (a common color scale was used between Figures 13 and 14 for both the concentrations and exceedance probabilities). The barrier indeed induces multiple perturbations on the wind and turbulence fields, decreasing the horizontal component of the mean wind, introducing a vertical velocity component by deflecting the wind streamlines, and increasing the turbulence and turbulent mixing. The algorithm PRIME within SCICHEM considers all these effects and allowed us to appreciate the increased dispersion that occurred due to the reduction in the odour concentration at the 1.7 m height. If the substance responsible for the odour presents no danger to human health or ecosystems, the increased dispersion and concentration reduction would not represent a cause of concern and the barrier could be considered effective for the reduction in the odour nuisance.

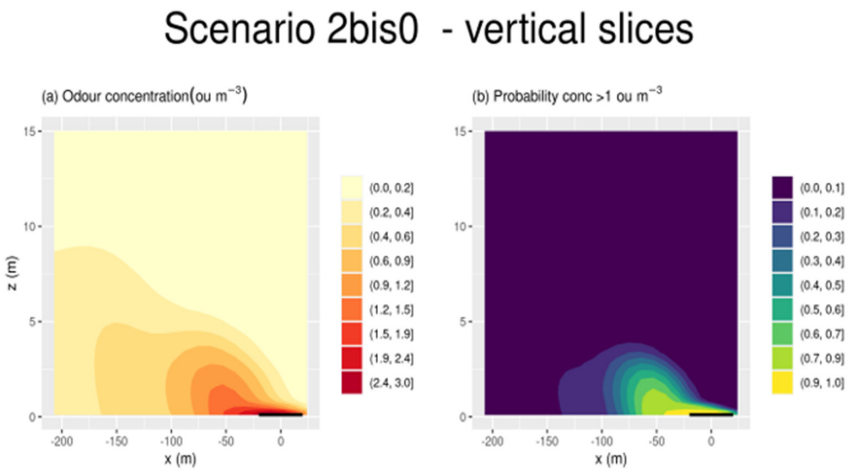

Figure 13. Vertical slices (x–z directions) of the odour concentrations (**a**) and exceedance probability of the 1 ou m^{-3} threshold (**b**) from the ground up to a 15 m height as simulated by SCICHEM. The meteorology and total emissions are the same as in the wind gust episode of scenario 2, but with the emission field replaced by a 40 m−diameter circular source, represented by a horizontal black line in the graphs. The coordinate x is expressed as the distance in meters from the center of the source, and z as the height in meters above the ground.

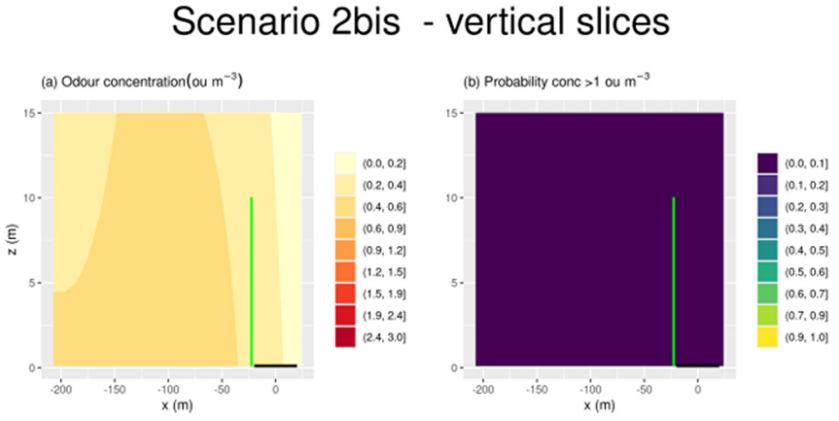

Figure 14. Vertical slices of the odour concentrations (**a**) and exceedance probability of the 1 ou m^{-3} threshold (**b**) from ground to a 15 m height as simulated by SCICHEM in the presence of a barrier (represented in green in the graphs). The meteorology and total emissions are the same as in the wind gust episode of scenario 2, but with the emission field replaced by a 40 m−diameter circular source, represented by a horizontal black line in the graphs. The coordinate x is expressed as the distance in meters from the center of the source, and z as the height in meters above the ground. The barrier is represented as a green rectangle.

Nevertheless, caution should be used when implementing barriers as a mitigation tool, especially if the emitted gases or particles could harm the environment and human health at very low concentrations in the far field and/or if a significant increase in the pollutant concentration in the immediate vicinity of the barrier occurs close to the ground. A similar concern arises in the industrial and urban context for areas close to stacks and buildings (building downwash). In these cases, optimal solutions could be vegetated barriers or specific materials that favor the deposition/capture of the pollutant, resulting in a net removal of the pollutant from the atmosphere. It should be noticed, however, that vegetation and porous structures in general do not act on the flow as non-permeable barriers, and this should be considered when selecting the modeling approach.

The PRIME algorithm was initially designed in the industrial context, but it contains all the physical mechanisms (plume rise, increase in turbulent mixing, etc.) induced by a barrier. Therefore, it is also applicable in the agricultural context with ground and passive sources. SCICHEM and PRIME could, therefore, be powerful tools in designing opportune barriers to reduce the odour nuisance, especially when the prevailing wind direction of the region/season and fertilizer application is known. It would be desirable to further develop the PRIME algorithm within SCICHEM in order to identify when the plumes are generated by area (and not only point) sources.

4. Conclusions

This work showed how dispersion modeling with a state-of-the-art research tool, such as the SCICHEM model, can support institutions in predicting and regulating odour nuisances while contributing to scientific research purposes and developing promising synergies between academic and regulatory works. The framework of the present project consisted of the Italian and international regulations on odours, and SCICHEM demonstrated the ability to inform and support decision-makers in estimating and regulating the odour concentrations and exceedance probabilities of specific thresholds. On the other hand, the use of the model in this context can potentially trigger new model developments for regulatory applications.

The results of our simulations, combined with the measurements of odour emissions using dynamic olfactometry, showed that a typical application of organic manure to an agricultural field of 2.4 ha can produce odour concentrations that exceed the minimal threshold identified by the national reference law up to a 500 m distance from the source. The most critical situation occurred in the vicinity of the source, under calm winds, stable conditions, and following the surface spreading method. The direct injection technique was highly performant in reducing the overall emissions and atmospheric concentrations. For intense winds, the plume elongated more than under light winds but with lower values of concentrations, as expected from the enhanced advection and mixing in these conditions.

The probability of exceeding the defined threshold of 1 ou m^{-3} was close to 0.7 on average at a distance of 500 m from the center for the field using the surface spreading technique, potentially raising a cause of concern from a regulatory point of view. On the other hand, we considered a very conservative scenario that included the following:

- The chosen threshold was the lowest considered by the Italian regulation.
- The emissions was considered constant during the whole month, thus constituting a "worst-case scenario" where fertilizer applications are either replicated very frequently or performed in neighbors' fields almost at the same time and for an extended period.

Considering the total emission rate (Table 3), we estimated a concentration/source ratio C/Q(s m^{-3}) in the direction of the prevailing wind. At approx. 400 m from the source, this ratio ranged between 10^{-6} s m^{-3} (unstable cases, see Figure 8) and 10^{-3} s m^{-3} (calm winds and stable conditions, see Figures 6 and 8). Our results were in line with previous findings ([40], Table 3) where the concentrations/source ratios were measured and simulated using different models. Even if the classification of the stable/unstable cases was finer in [40], the results were consistent with our C/Q ratios, being of the same order of magnitude, smaller for unstable cases, and larger for stable cases and calm winds.

The direct injection technique showed great mitigation potential, with a reduction in both the emissions and concentrations by a factor of two on average.

The concentrations observed during the calm wind episodes increased by a factor of 1.5 in their maximum values, while during the maximum wind gust event, the peak was reduced approximately by a factor of 4 as the odour plume reached greater distances. Additionally, the atmospheric stability had a great impact on the odour dispersion, with concentrations in the stable conditions being on average one order of magnitude larger than in the unstable conditions in the considered domain and at the sampling height of 1.7 m.

The PRIME algorithm in the model also allowed for the estimation of the effect of a barrier downwind from the source during the maximum wind gust event, showing a further reduction of approx. a factor 2.5 for the peak concentrations (close to the source), which became essentially zero for the exceeding probabilities averaged across the simulation domain. Even though this scheme is available only for point sources at present, we designed the source in the simulations to mimic the real field and the presence of the barrier as close as possible. The generalization of the algorithm for the area sources was identified as a promising perspective, particularly for applications in the agricultural context.

The results for the circular source with and without a barrier showed the strong potential of reducing odour concentrations in the vicinity of the source at the sampling height of 1.7 m. A vast literature exists on the potential of barriers in reducing the atmospheric dispersion of pollutants, both in urban/industrial and agricultural contexts [41]. Our results confirmed the promising mitigation potential of barriers against odour nuisances, especially if combining them with techniques that favor the capture or deposition of the pollutants upwind or within the barrier itself.

At the same time, our results showed how this reduction occurred along with the increased vertical mixing and dispersion. Optimal barriers for mitigation purposes should, therefore, be designed by considering several factors, including all the pollutant's characteristics and the region's prevailing meteorological conditions. If the odour compound emitted by the source is not harmful to human or ecosystem health, a slight increase in the vertical dispersion might be desirable as it reduces the level of human perception of the nuisance without causing major concern in the far-field region. On the contrary, if the substances causing the odour nuisance are atmospheric pollutants, the increase in horizontal and vertical dispersion might be a cause of concern. In these cases, better solutions are most likely vegetated barriers that can capture the particles/gases responsible for the odour nuisance. The combined effect on the wind, turbulence fields, and on the deposition of the pollutant would maximize the mitigation potential in these cases. Nevertheless, as long as only the odour nuisance is considered, the mitigation potential of the simulated barrier shown by our results was highly satisfactory.

Our results globally show the potential of using SCICHEM in the agricultural and regulatory context, particularly regarding odours, for its capability of simulating the exceedance probabilities and its implementation of the PRIME algorithm, since the use of barriers (either artificial or natural) is becoming a common practice to mitigate the dispersion of pollutants from various agricultural activities.

Author Contributions: Conceptualization, M.R.V., S.P. and M.A., software: M.R.V., validation: M.R.V., S.P., M.A. and B.T.; formal analysis, M.R.V., S.P., M.A. and B.T.; investigation, M.R.V., S.P., M.A. and B.T.; resources: S.P., M.A., G.B. and B.T.; data curation, S.P.; writing—original draft preparation, M.R.V.; writing—review and editing, M.R.V., S.P., M.A., A.P. and B.T.; visualization, M.R.V.; supervision, S.P.; project administration, S.P.; funding acquisition, S.P., M.A. and G.B. All authors have read and agreed to the published version of the manuscript.

Funding: This research was realized in the framework of the project PREPAIR (LIFE 15 IPE IT 013), funded by the EU programme LIFE.

Institutional Review Board Statement: Not applicable.

Informed Consent Statement: Not applicable.

Data Availability Statement: Not applicable.

Acknowledgments: We are thankful to the SCICHEM developers and researchers, in particular Douglas Henn, Eladio Knipping, Prakash Karamchandani, and Steven Schneider who provided guidance and precious suggestions for making the best use of the model. We are also grateful to David Iglesias Sánchez for his advice and assistance with graphics.

Conflicts of Interest: The authors declare no conflict of interest. The funders had no role in the design of the study; in the collection, analyses, or interpretation of the data; in the writing of the manuscript; or in the decision to publish the results.

Appendix A

The employed fertilizer was digestate, obtained from the anaerobic digestion of cattle slurry, poultry manure, and energy crops. The details about its chemical composition are given in Table A1, while Table A2 provides the amount applied to the experimental field.

Table A1. Digestate features.

Parameter	Value
Ammonia nitrogen (g/kg)	2.97
Total nitrogen (g/kg)	4.50
TAN (total ammonia nitrogen)/TKN (Total Kjeldahl Nitrogen) (%)	66.00
pH	7.30
Total phosphorus (g/kg)	2.35
Total potassium (g/kg)	3.05

Table A2. Digestate application features.

Parameter	Value
m^3 /ha applied	40.0
N applied (kg/ha)	180.0
N-NH_3 applied (kg/ha)	118.8

Appendix B

More than 50 models were reviewed in order to identify the suitable model for this study. The very first selection excluded the models that were evidently not suitable for the purpose (too computationally expensive, such as CFD models, or specific for only certain applications, such as pollutants from industrial stacks, road traffic, pesticides, radioactive compounds, etc.). The retained models were then characterized on the basis of 12 specific requirements and preference criteria. Therefore, this paper does not seek to provide a comprehensive review of the atmospheric dispersion models but to identify the most suitable model in the specific context of the project PrepAir, i.e., the model that presented the best balance among the capabilities for meeting the following criteria.

1. Representation of transport

The meteorological conditions and characteristics of atmospheric flow surrounding the sources are among the most important factors that determine odour intensity/concentration [42,43]. An accurate representation of these factors and the way they interact with the pollutant is, therefore, essential, and particular attention should be paid to the assumptions made in the model about pollutant/odour transport, the features of the underlying flow, as well as the capability of the model to ingest and process the detailed meteorological information from the field. The approaches to pollutant transport can be classified in four broad classes: the plume steady state (Gaussian or similar); the dynamic plume (puff models); Lagrangian;

and 3D Eulerian, with different approaches to solve or approximate a solution for the equation of advection–diffusion, hencewith different computational costs.

2. Possibility to model dispersion over complex terrain

"Complex terrain" generally refers to non-flat orography, in terms of the presence of hills or mountains. In these conditions, the model should be able to represent the distortion of the flow and tracer field. Even though the terrain in our simulated problem was flat, the possibility to model complex terrain was considered a preference criterion due to the potential of extending the model's applications.

3. Possibility to model dispersion across obstacles

Obstacles such as buildings and trees also create distortions in the flow at a smaller scale than complex orography, causing effects such as "building downwash" [44]. Accounting for the effects of these obstacles on the dispersion is usually needed in high-resolution, small-scale problems in both urban and rural environments, as well as considering that natural or artificial barriers can be used for their abatement potential [45,46]. Considering that both natural and artificial barriers are widely used in agriculture to mitigate dispersion, we considered the capability of representing the barriers as a preference criterion.

4. Possibility to model dry and wet deposition

Considering that odour compounds (both gaseous and aerosol) can be subject to both dry and wet deposition, the capability of representing these processes is generally considered an added value of the model. Nevertheless, in order to attain an accurate estimation of the compound of dry and wet deposition, several physico-chemical characteristics should be known and provided in the input to the models (e.g., the molecular diffusivity for gases, and the particles density and granulometry for aerosols).

5. Possibility to model chemical reactions and radioactive decay

This capability of the models can be generally considered as an advantage, especially when the chemical nature of the odour compounds is known.

6. Specific for odours or designed for tracers but applicable to odours

Odourous substances include many different compounds, either gases or aerosols. Over 160 chemical compounds have been identified in livestock wastes or in nearby air [47]. The models that are designed to represent the atmospheric dispersion of these compounds can also be, in principle, applied to odours [7]. Among the advantages of adopting a model that can be used for both odours and other tracers, we can mention the reduced costs (for purchase if applicable, installation, training, and computational resources). In some cases, specific odour modules are embedded in more general dispersion models. Additionally, methane or ammonia can be, under particular precautions, taken as a representative tracer for odours and they are simultaneously of high interest for agricultural emissions. The use of a common model for odours, gases, and particles emitted from agricultural sources could present an advantage for providing a common tool for an integrated assessment of the environmental, social, and climate impacts of farm operations, which can often be mitigated by means of similar abatement techniques (e.g., [48]). On the other hand, several important differences exist between odours and other tracers, including the different relevant timescales, the threshold-dependent character of odours, and the fact of not being subject to mass conservation. Particular precautions should be taken for dealing with these specificities of odours when choosing a dispersion model that was designed for other tracers.

The specific methods for considering the very short timescale fluctuations of concentrations are the following.

- Parametrization of the fluctuating plumes (a variant of the steady-state plume model) [49–52].
- Peak-to-mean schemes (applicable to both the plume and Lagrangian models).

Peak-to-mean approaches rely on particular assumptions on the concentration probability density function and parametrize the ratio of the peak/mean of this function. The peak-to-mean ratio can be parametrized in different ways, either by assuming a constant ratio or a ratio depending on the distance from the source, the source geometry, or the atmospheric stability [53]. In the choice of the model, we paid particular attention to the features that rendered the model suitable to treat these peculiarities of odours, still preferring a model that could also be used for other pollutants for the reasons mentioned above.

7. Type of source that can be modeled

Dispersion models can be designed to ingest input data either from emissions from very simple sources (e.g., point and continuous) or more complex sources (e.g., intermittent, volumetric). In addition, the flow from the source can either be regulated only by external atmospheric conditions (passive sources) or mechanically/ thermally forced (e.g., due to the presence of fans or the heating of the emitting apparatus). Our problem concerns the area source, approximated as continuously emitting. Nevertheless, the capability of the models to represent more complex sources was considered as a preference criteria for the potential to extend the applications to other situations.

8. Spatial scale of applicability

Certain source types, in specific atmospheric conditions, produce odours that can be clearly perceived at distances of 100 km or more [54]. However, in most applications on agricultural operations, the relevant scale for odour perception is a few kilometers. Therefore, the applicability of the model to such a scale was considered as a requirement. The spatial resolution of the model, if applicable, should consider the variation of the meteorological and topographical data as the input.

9. Time step and averaging interval

In Eulerian, Lagrangian, and puff models, the computation time step is the interval of time used for solving the equations of motion. In both the dynamic and steady-state models, the time scale at which the pollutant is sampled or averaged is also relevant (it generally corresponds to the time resolution of the model's output). The typical time scale for odour perception (a few seconds) is usually much shorter than the typical time scale used for monitoring and modeling other pollutants (usually 10 min to one hour). This means that the concentrations peaks that are responsible for odour perception will be generally smoothed out in the output. The dispersion models that integrate specific methods to consider the instantaneous fluctuations of the concentrations with specific statistical methods have been given a high preference in our selection process.

10. Applied in regulatory context

Dispersion models are often used by regulatory agencies to assess either the actual or potential impacts on the area surrounding agricultural, urban, or industrial facilities. The objectives can be multiple, including supporting authorization procedures, elaborating/applying appropriate control/abatement techniques, or defining setback distances. There has been an increasing attention towards odours in the last 30 years, with the adoption of dedicated regulations in many countries [20,55–57]. However, consolidated national and international frameworks for detecting, modeling, and managing odours are still lacking. The acknowledgement from regulatory agencies for a model that is suitable for these purposes is considered a preference criteria.

11. License

Organizations that develop and maintain the models can apply different policies on them, keeping the model as proprietary and distributing it only as executable (with or free of charge) or making both the model's executable and sources available at no cost under specific public licenses that regulate their use and modifications. The last category was preferred in our selection process.

12. Existence of a user manual, graphical user interface, and technical documentation

The availability of a user manual and a graphical user interface (GUI) have been considered as an important preference criteria. These elements strongly reduce the time and economic resources needed for initial training and the need for scientific–technical support from the organizations that develop and maintain the model. Considering that the model should be suitable for both normative and scientific purposes, a comprehensive, freely available, and updated technical documentation should also be available in order to provide a strong and clear scientific basis of the simulation results.

The following models have been retained after a first selection and characterized according to the listed criteria.

Appendix B.1. Steady-State Plume Models

Plume models calculate pollutant concentrations and assume the steady conditions of the underlying flow and emissions during the simulation/output timestep and homogeneous statistical properties of the flow across the modeling domain. The typical sampling/integration periods of these models range between 10 min and 1 h. Most commonly used plume models use a Gaussian solution of the advection–diffusion equation in steady conditions, but variants of this functional are also possible. Steady-state plume models are generally simpler and computationally less demanding than dynamic Eulerian and Lagrangian models. The computational cost of these models can be generally considered as "low".

Appendix B.1.1. AERMOD

The AMS/EPA Regulatory Model (AERMOD) [58] is a steady state Gaussian model, formulated and widely used in regulatory contexts (it is the U.S. Environmental Protection Agency regulatory model).

1. Representation of transport: Convective and stable conditions are represented by different parametrizations of micrometerological parameters (L, u*, w*) and stability functions. The wind profile is assumed to be logarithmic. The pollutant plume is represented by Gaussian functions. In the CBL (convective boundary layer), the plume is represented as bi-Gaussian in z (vertical dispersion) and Gaussian in y (horizontal dispersion). In the SBL, both the horizontal and vertical shapes are assumed to be Gaussian. The pollutant plume is the weighted sum of a "horizontal plume" (terrain impacting) and a "terrain following" plume.
2. Possibility to model dispersion over complex terrain: Yes.
3. Possibility to model dispersion across obstacles: AERMOD can represent the effect of building wakes on the plumes through the incorporation of the PRIME algorithm (plume rise model enhancements).
4. Possibility to model dry and wet deposition: Yes.
5. Possibility to model chemical reactions and radioactive decay: Radioactive decay only.
6. Specific for odours or designed for tracers but applicable to odours: AERMOD was designed for tracers, but has also been used for odours in several studies [59,60].
7. Type of source that can be modeled: AERMOD can handle point, line, area, and volume sources, eventually with buoyancy effects.
8. Spatial scale of applicability: As most of the steady-state Gaussian models, AERMOD assumes the homogeneous properties of the flow across the modeling domain. Therefore, the spatial scale of applicability is of a few km.
9. Time step and integration interval: Minimum sampling interval is one hour.
10. Applied in regulatory context: AERMOD was formulated and has been widely used in regulatory contexts, being the reference U.S. Environmental Protection Agency regulatory model [61].
11. License: Software is available at no cost.

12. Existence of a user manual, graphical user interface, and technical documentation: Yes. Website: https://www.epa.gov/scram/air-quality-dispersion-modeling-preferred-and-recommended-models#aermod (URL accessed on 14 February 2023)

Appendix B.1.2. ADMS

The Atmospheric Dispersion Modelling System (ADMS) is a Gaussian dispersion model designed for representing pollutant dispersions from industrial sources, but it has also been used for odours.

1. Representation of transport: Convective and stable conditions are represented by different parametrizations of micrometerological parameters (L, u*, w*), and stability functions. The pollutant plume is represented by Gaussian functions and skewed distributions in the CBL. The effects of the buoyant plume rise can be modeled. The ADMS also includes a "puff" module.
2. Possibility to model dispersion over complex terrain: Yes.
3. Possibility to model dispersion across obstacles: Yes.
4. Possibility to model dry and wet deposition: Yes.
5. Possibility to model chemical reactions and radioactive decay: Yes.
6. Specific for odours or designed for tracers but applicable to odours: ADMS was designed for tracers but has been used for odours in several studies, and contains a dedicated odour module [59,62].
7. Type of source that can be modeled: ADMS can handle point, line, area, and volume sources.
8. Spatial scale of applicability: Different versions of the model exist, optimized for various contexts and spatial scales (ADMS-Roads, ADMS-Urban, ADMS-Airport). The maximum spatial scale is limited by the hypothesis of the horizontal homogeneity. It is, therefore, limited to the short range, i.e., a few km. Nevertheless, a specific version of the model has been developed for nesting the ADMS to regional models (ADMS-Urban regional model).
9. Time step and averaging interval: Integration time interval is 1 h.
10. Applied in regulatory context: ADMS is widely used in regulatory contexts (e.g., UK Health and Safethy Executive, Environment Agency in England, Scottish Environmental Protection Agency, Northern Ireland Environment Agency, Natural Resources Wales, Food Standards Agency of the United Kingdom).
11. License: Proprietary, charges on distribution.
12. Existence of a user manual, graphical user interface, and technical documentation: Yes. Website: https://www.cerc.co.uk/environmental-software/ADMS-model.html (URL accessed on 14 February 2023)

Appendix B.1.3. CDTMPLUS

The EPA Complex Terrain Dispersion Model (CDTMPLUS) is a Gaussian, steady state dispersion model particularly designed for modeling dispersion over complex terrains.

1. Representation of transport: The pollutant plume is represented by Gaussian functions. In the CBL (convective boundary layer), the plume is represented as skewed, bi-Gaussian in z (vertical dispersion), and Gaussian in y (horizontal dispersion). In the SBL, both the horizontal and vertical shapes are assumed to be Gaussian. The effects such as the buoyant or mechanical plume rise can be modeled, as well as the partial plume penetration into elevated stable layers.
2. Possibility to model dispersion over complex terrain: The effects of very complex terrains can be modeled with a dedicated preprocessor which needs a 3D description of the terrain as the input.
3. Possibility to model dispersion across obstacles: Yes.
4. Possibility to model dry and wet deposition: Yes.
5. Possibility to model chemical reactions and radioactive decay: No.

6. Specific for odours or designed for tracers but applicable to odours: No reference was found about use of CDTMPLUS for odours.
7. Type of source that can be modeled: Only point.
8. Spatial scale of applicability: Short range (< 5 km).
9. Time step and averaging interval: Integration time step 1 h.
10. Applied in regulatory context: CDTMPLUS has been widely used in regulatory contexts and is listed among the "preferred and recommended models" of the U.S. Environmental Protection Agency [27] for air quality dispersion modeling.
11. License: Software is available at no cost.
12. Existence of a user manual, graphical user interface, and technical documentation: Yes. Website: https://www.epa.gov/scram/air-quality-dispersion-modeling-preferred-and-recommended-models#ctdmplus (URL accessed on 14 February 2023)

Appendix B.1.4. FIDES

The Flux Interpretation by Dispersion and Exchange over the Short-range model (FIDES) [63,64] is a steady-state plume dispersion model widely used in agricultural contexts. It was designed for ammonia, but is also used for pesticides [65].

1. Representation of transport: The functional form of the plume is taken from [66], a variant of the classical Gaussian shape, and the wind profiles are assumed to follow a power law. The meteorological data in the input (hourly time step) include the wind direction, roughness length z0, Obukhov length L, and friction velocity u*. L, z0, and u* can be either given as the input or calculated by the model from the wind, temperature, and canopy height data.
2. Possibility to model dispersion over complex terrain: No.
3. Possibility to model dispersion across obstacles: No.
4. Possibility to model dry and wet deposition: Yes.
5. Possibility to model chemical reactions and radioactive decay: No.
6. Specific for odours or designed for tracers but applicable to odours: No reference was found about use of FIDES for odours.
7. Type of source that can be modeled: Point, line, area, and volume sources, continuous and discontinuous.
8. Spatial scale of applicability: local scale, < 5 km.
9. Time step and averaging interval: The integration time is 30 min.
10. Applied in regulatory context: No reference was found about use of FIDES in regulatory contexts.
11. License: The FIDES software is distributed at no cost.
12. Existence of a user manual, graphical user interface, and technical documentation: The model can be used with the following languages: visual basic, R, Matlab, and C, but no dedicated GUI is available. A succinct user manual is available. Website: https://www6.versailles-grignon.inrae.fr/ecosys_eng/Productions/Softwares-Models/FIDES2 (URL accessed on 14 February 2023)

Appendix B.1.5. OdiGauss

OdiGauss [67] is a free software specifically designed to estimate odour dispersion from multiple point sources and to generate the related maps. It can be coupled to a model of odour emissions from poultry farms (EmiFarm).

1. Representation of transport: OdiGauss is a steady-state Gaussian plume model, implementing [68] parametrizations for the plume functional form and dispersion coefficients. It accounts for the atmospheric stability through the Pasquill classes, and for calm wind (wind speed <0.5 m/s) with a dedicated algorithm, similar to the ISCST3 model or the Cirillo–Poli model [69].
2. Possibility to model dispersion over complex terrain: No.
3. Possibility to model dispersion across obstacles: No.

4. Possibility to model dry and wet deposition: A corrective coefficient is applied in the occurrence of rain to consider the phenomenon of odour removal due to "scavenging".
5. Possibility to model chemical reactions and radioactive decay: No.
6. Specific for odours or designed for tracers but applicable to odours: The model OdiGauss has been specifically designed for odours, implementing a peak-to-mean correction to the average output concentrations. A constant value of the peak-to-mean ratio is adopted, which may be tuned to follow a precautionary criterion. The suggested default value is equal to 2.3, while a value of one disables the peak-to-mean correction.
7. Type of source that can be modeled: The model can either ingest constant emission rates, or variable, multiple, and more complex emissions as modeled by the EmiFarm model, also included in the OdiGauss package. EmiFarm simulates odour emissions from poultry manure heaps.
8. Spatial scale of applicability: Short range (<5 km).
9. Time step and averaging interval: Integration period is one hour.
10. Applied in regulatory context: Applied in the context of environmental authorization procedures (e.g., [70]).
11. License (proprietary—charges on distribution/ proprietary—distributed at no cost/open source): Software publicly available at no cost.
12. Existence of a user manual, graphical user interface, and technical documentation: Yes. Website: http://semola.uniud.it/projects/odigauss/ (URL accessed on 13 February 2022)

Appendix B.2. Lagrangian Models

Lagrangian models solve the equation for the motion of tracers and particles in fluids, namely the Langevin equation. The main advantage of Lagrangian models compared to Gaussian models is the possibility of dealing explicitly with non-steady conditions. When compared to Eulerian models, they exhibit an independence from spatial grid, absence of numerical diffusion, and generally better performance close to the sources. The reviews of the application of a Lagrangian approach to atmospheric dispersion can be found in [71,72]. Lagrangian models are computationally more expensive than steady-state plume models due to the dynamic approach and the need to follow a large number of particles for each integration time. Generally, it is considered that the release of ~10^5 particles is needed to mimic an emission episode with a statistical significance. The computational cost of these models can be generally considered as "medium".

Appendix B.2.1. WindTrax

WindTrax [73,74] is a Lagrangian stochastic particle dispersion model that is strictly applicable for passive trace gases, but it has also been used for aerosols and odours. It has been widely validated and applied in agricultural contexts, both in forward and backward modes. It possesses a sound and well-documented scientific basis, a user-friendly interface, and a low computational cost.

1. Representation of transport:

WindTrax calculates dispersion by mimicking the trajectories of numerous tracer "particles" as they travel in the atmosphere. Langevin equations are used to calculate the trajectories, and the model can be applied in either forward or backward modes (for estimating the concentrations from emissions, and vice versa). Gas concentrations (or the emission fluxes when used in the backward mode) are calculated using statistical techniques at the end of the simulation averaging time (which is typically 10 to 60 min). The users sets the number of particle trajectories used in the simulation. A higher number of released particles reduces the uncertainty of the model results but requires a greater computation time. While the recommended number of model particles varies with the source-to-sensor distance and geometry, 10^5 particles is often sufficient. The meteorological conditions are assumed to be horizontally homogeneous and temporally stationary during

the simulation averaging period (10–60 min). The underlying surface layer wind flow is assumed to follow the Monin–Obukhov similarity theory, and the mean wind and turbulence profiles are defined by the friction velocity, the Obukhov length, and the surface roughness length. These input properties can be directly measured or inferred from a single meteorological station. WindTrax also presents the possibility of ingesting various types of input meteorological/micrometeorological data, including first and second moments of high frequency wind records from a sonic anemometer.

2. Possibility to model dispersion over complex terrain: No.
3. Possibility to model dispersion across obstacles: No.
4. Possibility to model dry and wet deposition: No, the surface is assumed to be reflective. In a Lagrangian model, this means that particle trajectories intersecting the surface are "reflected" back into the flow. A version of the software with deposition has also been developed, but at present it is used for research purposes and not publicly available.
5. Possibility to model chemical reactions and radioactive decay: No.
6. Specific for odours or designed for tracers but applicable to odours: Windtrax does not include specific modules for odours, but has been applied in this context either by using methane as a tracer and indicator of the odour concentration [75] or directly simulating the odour concentrations in ou/m^3 [76].
7. Type of source that can be modeled: Point, line, area, and volume sources can be modeled. Non-steady emissions can be handled if the timescales of their variations is longer than the model integration period (30 min).
8. Spatial scale of applicability: The WindTrax model is a short-range model, applicable to distances less than approximately 5 km from a gas source. It is a surface layer model and errors can be expected at larger downwind distances as (1) trajectories may travel above the surface layer and then descend back into the surface layer, (2) assumptions of horizontal homogeneity of the wind may be violated, and (3) assumptions of stationarity in the wind can be violated.
9. Time step and averaging interval: The model averaging time is generally set between 10 and 60 min, meaning that the meteorological and emission data should be provided at this frequency, and the output concentration will be averaged on this time interval. The internal model timestep (for solving the Langevin equations) is instead specified as a certain fraction of the Lagrangian time scale (typically <1 s) and is calculated according to the flow characteristics [74].
10. Applied in regulatory context: WindTrax has been accepted for regulatory reporting purposes. T.K. Flesch (personal communication) reports that WindTrax has been used in Canada for regulatory reporting of methane and carbon dioxide emissions from industry.
11. License: WindTrax is a proprietary software (Thunder Beach Scientific) but freely available and distributed at no cost.
12. Existence of a user interface and manual (y/n): Yes. Website: http://www.thunderbeachscientific.com/ (URL accessed on 14 February 2023)

Appendix B.2.2. SPRAY

SPRAY [77–79] is a Lagrangian stochastic particle dispersion model designed for gases and aerosols, but also used for odours. It has been validated against many test cases, both in controlled conditions (such as wind tunnel experiments) and in real atmosphere, flat, and complex terrain with or without explicitly considering the presence of buildings.

1. Representation of transport:. The model solves the Langevin equation to follow the trajectories of a certain number of particles released for each emission episode. The turbulent flow can be parametrized as Gaussian, with velocity fluctuations depending on the atmospheric stability, according to [68]. In addition, the model contains several schemes for considering non-Gaussian, skewed velocity distributions and non-stationary flows.

It presents the possibility to ingest highly detailed meteorological information, such as wind data from ultrasonic anemometers or SODAR (SOnic Detection And Ranging) for the internal calculation of turbulent parameters. Alternatively, these parameters can be estimated from classic anemometer measurements.

2. Possibility to model dispersion over complex terrain: Yes.
3. Possibility to model dispersion across obstacles: Yes, in the "microscale version" of the model (PSPRAY).
4. Possibility to model dry and wet deposition: Yes.
5. Possibility to model chemical reaction/radioactive decay: Only radioactive decay in the SPRAY version and simplified chemical mechnisms for NO_x/NO_2 transformation (PSPRAY version).
6. Specific for odours or designed for tracers but applicable to odours: SPRAY and PSPRAY have been used for odours and implement a specific module for odours (peak-to-mean) derived from [80] based on the original work of [81,82]. Both SPRAY and PSPRAY have been tested for odour dispersion [79].
7. Type of source that can be modeled: Point, line, area, and volume sources, continuous and discontinuous. Both passive and momentum or buoyancy forced emissions can be modeled.
8. Spatial scale of applicability, spatial resolution if applicable: From micro (1 km) to regional scales.
9. Time step: Both time step and integration interval are variable, depending on the meteorological and emission conditions.
10. Applied in regulatory context: SPRAY has been applied in several cases for regulatory and environmental impact assessment purposes [83,84].
11. License: Proprietary.
12. Existence of a graphical user interface and manual: Yes. Website: https://www.aria-net.it/it/prodotti/spray/ (URL accessed on 14 February 2023)

Appendix B.2.3. FLEXPART

The FLEXible PARTicle dispersion model (FLEXPART) [85] is a Lagrangian dispersion model that can be used both in forward and backward modes. It has been widely used and validated in different contexts and spatio-temporal scales.

1. Representation of transport: FLEXPART assumes a default underlying Gaussian turbulence and parametrizations of velocity fluctuations depending on the atmospheric stability, according to [68]. However, it contains options to switch to non-Gaussian, skewed velocity distributions [86]. The model handles deep convection by using the [87] scheme.
2. Possibility to model dispersion over complex terrain: Yes.
3. Possibility to model dispersion across obstacles: Yes.
4. Possibility to model dry and wet deposition: Yes.
5. Possibility to model chemical reaction/radioactive decay: Radioactive decay only.
6. Specific for odours or designed for tracers but applicable to odours: FLEXPART was designed for gases and particles, but has also been used for odours in some specific applications (e.g., [88]).
7. Type of source that can be modeled: Point, line, area, or volume sources can be modeled.
8. Spatial scale of applicability, spatial resolution if applicable: Local to global, but more frequently used for mesoscale problems.
9. Time step: Time step is variable, depending on the the flow conditions.
10. Applied in regulatory context: FLEXPART has been widely used in regulatory contexts, including the reconstruction of the Chernobyl accident, and the estimation of halocarbon emissions (regulated by the Montreal Protocol).
11. License: Publicly available and open source, released under the GNU General Public License.
12. Existence of a user manual, graphical user interface, and technical documentation: Yes. Website: https://www.flexpart.eu/ (URL accessed on 14 February 2023)

Appendix B.2.4. HYSPLIT

The Hybrid single-particle Lagrangian integrated trajectory model (HYSPLIT) is a hybrid Eulerian–Lagrangian, multiscale model from local to global scale [89].

1. Representation of transport: HYSPLIT combines Lagrangian and Eulerian approaches by using of a moving frame of reference for the advection—diffusion calculations and a fixed three-dimensional grid as the frame of reference to compute the pollutant concentrations. The model can be used for simulating either particles or "puffs", both in forward and backwards modes.
2. Possibility to model dispersion over complex terrain: Yes, limited to what is resolved by the meteorological model's terrain.
3. Possibility to model dispersion across obstacles: No.
4. Possibility to model dry and wet deposition: Yes.
5. Possibility to model chemical reaction/radioactive decay: Yes.
6. Specific for odours or designed for tracers but applicable to odours: Designed for gases and particles, but has also been used for odours (e.g., [90,91]).
7. Type of source that can be modeled: Point and area sources, instantaneous or continuous.
8. Spatial scale of applicability: Local to continental.
9. Time step and averaging interval: Time step is variable, depending on the the flow conditions. Minimum value for the time step is 1 min.
10. Applied in regulatory context: HYSPLIT has been used in several cases for regulatory purposes, for example in emergency response and the reconstruction of nuclear accidents, such as Chernobyl and Fukushima.
11. License: HYSPLIT sowtware is publicly available and distributed at no cost.
12. Existence of a user manual, graphical user interface, and technical documentation: Yes. Website: https://www.ready.noaa.gov/HYSPLIT.php (URL accessed on 14 February 2023)

Appendix B.2.5. AUSTAL2000

AUSTAL2000, a Lagrangian dispersion model, is the reference model for the German Regulation on Air Quality Control.

1. Representation of transport: AUSTAL2000 is a stochastic Lagrangian dispersion model simulating particle trajectories by solving the Langevin equation and sampling them at the receptor location by using statistical techniques. The input data that are used by the model to represent the underlying flow include the roughness length, wind measurement height, wind direction, wind speed, and stability classes, according to Klug–Manier (analogous of the Pasquill stability classes).
2. Possibility to model dispersion over complex terrain: Yes.
3. Possibility to model dispersion across obstacles: Yes.
4. Possibility to model dry and wet deposition: Dry deposition is handled.
5. Possibility to model chemical reactions and radioactive decay: Yes.
6. Specific for odours or designed for tracers but applicable to odours: AUSTAL2000 contains an aerosol module (peak-to-mean) for making predictions about the frequency of odour nuisance.
7. Type of source that can be modeled: Point, line, area, and volume, constant or variable, with or without buoyant rise. Multiple sources can be handled by the model.
8. Spatial scale of applicability: Up to 50 km.
9. Time step and averaging interval: Variable time step according to the flow characteristics, integration interval of 1 h.
10. Applied in regulatory context: Yes, formulated and applied in regulatory context in Germany.
11. License: The program package AUSTAL2000, including the source code, is distributed free of charge. The programs and source code are subject to the GNU Public Licence.
12. Existence of a user manual, graphical user interface, and technical documentation: Yes. Website: http://www.austal2000.de/en/home.html (URL accessed on 14 February 2023)

Appendix B.3. Puff Models

Puff models simulate emissions as a succession of puffs, i.e., discrete packets of pollutant material, which, after release, move according to the Lagrangian trajectories and, within a short time after release, can be approximated by an evolving Gaussian shape [92,93]. Compared to the LS particle models, puff models are generally less expensive in terms of computational resources, as a large number of the simulated particles are replaced by individual puffs. On the other hand, by solving the trajectory equations dynamically, they are more expensive than the steady-state plume models. The overall concentration is obtained by integrating the concentration distributions of each puff during the sampling time step. By explicitly including the time evolution of the concentrations, puff models are more suited for dealing with temporally and/or spatially varying flow fields, complex terrain, non-uniform land use patterns, coastal effects, stagnation conditions characterized by calm or very low wind speeds, and variable wind directions. The computational cost of these models can be generally considered "medium".

Appendix B.3.1. CALPUFF

The California Puff Model (CALPUFF) is an air quality modeling system for regulatory use, developed by the Sigma Research Corporation (now part of Earth Tech, Inc.). The CALPUFF modeling system includes three main components: CALMET, CALPUFF, and CALPOST (post-processing). In the simplest terms, CALMET is a meteorological preprocessor for the preparation of hourly wind and temperature fields on a three-dimensional gridded modeling domain. In the simplest configuration, CALPUFF can use simpler non-gridded meteorological data from a single station.

1. Representation of transport: CALPUFF is a multi-layer, non-steady state puff model. The puffs growth is parametrized by vertical and horizontal dispersion coefficients (sigma_z and sigma_y) according to the different locations and stability conditions, namely the surface, mixed, and entrainment layers and the neutral, stable, and convective conditions [94]. It can take into account nonsteady meteorological conditions and situations of slow or no wind. CALPUFF can also handle buoyant and momentum plume rises, partial penetration into an elevated inversion layer, plume fumigation, vertical wind shear, and other effects.
2. Possibility to model dispersion over complex terrain: Yes.
3. Possibility to model dispersion across obstacles: Yes.
4. Possibility to model dry and wet deposition: Yes.
5. Possibility to model chemical reaction/radioactive decay: Yes.
6. Specific for odours or designed for tracers but applicable to odours: CALPUFF has been applied to odour dispersion in several studies [95–97]. Some intercomparison exercises outlined CALPUFF's better performances with respect to other commonly used dispersion models in the context of odours [98,99].
7. Type of source that can be modeled: Point, line, area, and volume sources, both constant and varying, passive and active (with buoyant or momentum rise).
8. Spatial scale of applicability: From tens of meters to hundreds of kilometers.
9. Time step and averaging interval: Averaging times from one hour to one year.
10. Applied in regulatory context: Yes.
11. License: Proprietary. Model codes and associated processing programs are provided by Exponent, Inc. with a no-cost, limited-use license.
12. Existence of a graphical user interface and manual: Yes. Website: http://www.src.com/ (URL accessed on 14 February 2023)

Appendix B.3.2. SCIPUFF/SCICHEM

The Second-order Closure Integrated PUFF (SCIPUFF) [100] is a non-steady-state, second-order closure integrated puff model. The Second Order Closure Integrated Puff Model with Chemistry (SCICHEM) [20,21], which stands for SCIPUFF with CHEMistry,

implements some additional chemistry modules and has the advantage of being an open source model.

1. Representation of transport: SCIPUFF/SCICHEM can represent time-dependent, inhomogeneous flows in different stability conditions with shear distortions or non-linear phenomena such as buoyant and mechanical rise dynamics. The model has been widely tested in laboratory conditions and short-range and continental scale field experiments. The turbulent diffusion parameterization in SCIPUFF is based on the second-order turbulence closure theory, which relates the dispersion rate to the velocity fluctuation statistics. In addition to the average concentration value, the closure model provides a prediction of the statistical variance in the concentration field resulting from the random fluctuations in the wind field. The model allows for the estimation of the variance and probability distribution for the predicted value, and as such, it is naturally well suited for simulating odours.
2. Possibility to model dispersion over complex terrain: Yes.
3. Possibility to model dispersion across obstacles: Yes.
4. Possibility to model dry and wet deposition: Yes.
5. Possibility to model chemical reactions and radioactive decay: Yes (integrated with SCICHEM).
6. Specific for odours or designed for tracers but applicable to odours: SCIPUFF has been designed for gases and aerosols but it has also been used with odours [101]. Moreover, the second-order closure scheme provides a natural framework for predicting the concentration fluctuations, which are relevant for odours (in addition to the mean value).
7. Type of source that can be modeled: Point, line, area, volume, continuous and variable, moving sources, multiple sources, eventually with momentum or buoyancy rise.
8. Spatial scale of applicability: Laboratory to continental.
9. Time step and averaging interval: SCIPUFF/SCICHEM uses an adaptive timestep, according to the characteristics of the flow.
10. Applied in regulatory context: SCIPUFF was approved in 1995 by the U.S. Environmental Protection Agency as an "alternative model" for pollutant dispersion [27] and it constitutes the dispersion model component in two U.S. Department of Defense modeling systems.
11. License (proprietary—charges on distribution/ proprietary—distributed at no cost/ open source): SCIPUFF is proprietary, while SCICHEM is a public domain source model.
12. Existence of a user interface and manual: Yes. SCICHEM available at https://github.com/epri-dev/SCICHEM (URL accessed on 14 February 2023)

Appendix B.3.3. INPUFF

The integrated PUFF model (INPUFF) is a non-stationary puff model capable of managing a large number of sources and receptors.

1. Representation of transport: In the INPUFF model, the Gaussian dispersion equation is used at each time step to calculate the contribution to the concentration at each receptor from each puff. In the default configuration, the model assumes homogeneous and constant wind conditions, but the user can specify the wind at each time step and up to 100 locations in the domain. The model incorporates three different dispersion algorithms, and the user can eventually link the model to alternative dispersion modules.
2. Possibility to model dispersion over complex terrain: Yes.
3. Possibility to model dispersion across obstacles: No.
4. Possibility to model dry and wet deposition: Dry deposition only.
5. Possibility to model chemical reactions and radioactive decay: No.
6. Specific for odours or designed for tracers but applicable to odours: INPUFF was developed for gases and aerosols but it has also been used for odours.

7. Type of source that can be modeled: The model can represent point sources, continuous and non-continuous, fixed or in motion, both passive and active. It is capable of managing multiple sources.
8. Spatial scale of applicability: From tenths of meters to tenths of kilometers.
9. Time step and averaging interval: The computation timestep is variable, according to the atmospheric flow conditions. The minimum integration timestep is one hour.
10. Applied in regulatory context: INPUFF has been developed in regulatory context. Despite not being officially recommended by the most known environmental agencies, it has been largely used for the analysis of environmental accidents and for evaluating the impacts of industrial activities.
11. License: Proprietary.
12. Existence of a user interface and manual: Yes. Website: https://cfpub.epa.gov/si/si_public_record_Report.cfm?Lab=ORD&dirEntryId=47242 (URL accessed on 14 February 2023).

Appendix B.4. Eulerian Chemistry Transport Models

Eulerian models for atmospheric dispersion numerically solve the continuity equation for the concentration of a given atmospheric component over a certain spatial domain and 3D grid. These models can be highly demanding in terms of computational resources, especially for large domains and/or high spatial/temporal resolutions.

Generally, they require a wide set of input data, including emissions, orography, and 3D meteorological fields.

The computational cost of these models can be generally considered "high".

Appendix B.4.1. CMAQ

The Community Multiscale Air Quality modeling system (CMAQ) is an active open-source development project of the U.S. EPA that consists of a suite of programs for conducting air quality model simulations. The model can assimilate and process the input meteorological data from the WRF (weather research and forecasting) model in an offline mode or an one-way or two-way mode online. In the first case, the WRF fields are produced beforehand. In the second and third case, the two models are instead coupled, respectively, without and with the feedback of the atmospheric chemistry on the meteorological fields.

1. Representation of transport: The CMAQ is a 3D Eulerian model that numerically solves the advection–diffusion equations while maintaining the chemical reactions.
2. Possibility to model dispersion over complex terrain: Yes.
3. Possibility to model dispersion across obstacles: No specific calculation for building-sized obstacles. Moreover, the typical resolution of the model (>1 km) does not allow for the evaluation of this type of phenomena.
4. Possibility to model dry and wet deposition: Yes, both dry and wet deposition.
5. Possibility to model chemical reactions and radioactive decay: The CMAQ implements advanced schemes for photochemical reactions and non-linear chemistry.
6. Specific for odours or designed for tracers but applicable to odours: We didn't find any reference about the use of the CMAQ for odours.
7. Type of source that can be modeled: Any type of source that is compatible with the spatial grid of the model and its temporal resolution.
8. Spatial scale of applicability: The CMAQ is a multiscale model and it can be applied to urban and emisphere-scale problems.
9. Time step and averaging interval: Can be adjusted according to the spatial resolution.
10. Applied in regulatory context: The CMAQ has been formulated and widely used in regulatory context.
11. License: Public domain source model.
12. Existence of a user interface and manual: Yes. Website: http://www.epa.gov/cmaq (URL accessed on 14 February 2023)

Appendix B.4.2. CALGRID

The California grid model (CALGRID) is a photochemical Eulerian model developed by the researchers of Sigma Research Corporation (today part of Earth Tech), as an update to the UAM-IV model. To date, it is maintained by the California Air Resources Board (CARB).

1. Representation of transport: CALGRID is a 3D Eulerian model that includes several schemes for horizontal and vertical transport. In particular, the [102] advection scheme ensures mass conservation and minimizes the numerical diffusion. CALGRID presents several possibilities for vertical spacings.
2. Possibility to model dispersion over complex terrain: Yes.
3. Possibility to model dispersion across obstacles: No specific calculation for building-sized obstacles. Moreover, the typical resolution of the model (>1 km) does not allow for the evaluation of this type of phenomena.
4. Possibility to model dry and wet deposition: Yes, both dry and wet deposition.
5. Possibility to model chemical reactions and radioactive decay: Yes, also photochemical reactions.
6. Specific for odours or designed for tracers but applicable to odours: No references were found about the use of CALGRID for odours.
7. Type of source that can be modeled: Any type of source that is compatible with the spatial grid of the model and its temporal resolution.
8. Spatial scale of applicability: Multiscale model, applicable from the urban to the continental scale. Horizontal resolution can be adjusted and typically ranges between 1 and 5 km.
9. Time step and averaging interval: Adjustable according to the spatial resolution.
10. Applied in regulatory context: CALGRID has been widely used for regulatory purposes, in particular for assessments of ozone control strategies.
11. License: Proprietary.
12. Existence of a user interface and manual: Yes. Website: http://www.arb.ca.gov/research/research-results.php (URL accessed on 14 February 2023)

References

1. Leonardos, G.; Kendall, D.; Barnard, N. Odour threshold determination of 53 odourant chemicals. *J. Environ. Conserv. Eng.* **1973**, *3*, 579–585. [CrossRef]
2. Hayes, E.T.; Curran, T.P.; Dodd, V.A. A dispersion modelling approach to determine the odour impact of intensive poultry production units in Ireland. *Bioresour. Technol.* **2006**, *97*, 1773–1779. [CrossRef] [PubMed]
3. Brancher, M.; Griffiths, K.D.; Franco, D.; de Melo Lisboa, H. A review of odour impact criteria in selected countries around the world. *Chemosphere* **2017**, *168*, 1531–1570. [CrossRef] [PubMed]
4. Liang, Z.S.; Zhang, L.; Wu, D.; Chen, G.H.; Jiang, F. Systematic evaluation of a dynamic sewer process model for prediction of odour formation and mitigation in large-scale pressurized sewers in Hong Kong. *Water Res.* **2019**, *154*, 94–103. [CrossRef] [PubMed]
5. Zilio, M.; Orzi, V.; Chiodini, M.; Riva, C.; Acutis, M.; Boccasile, G.; Adani, F. Evaluation of ammonia and odour emissions from animal slurry and digestate storage in the Po Valley (Italy). *Waste Manag.* **2020**, *103*, 296–304. [CrossRef]
6. Witherspoon, J.R.; Adams, G.; Cain, W.; Cometto-Muniz, E.; Forbes, B.; Hentz, L.; Novack, J.T.; Higgins, M.; Murthy, S.; McEwen, D.; et al. Water Environment Research Foundation (WERF) anaerobic digestion and related processes, odour and health effects study. *Water Sci. Technol.* **2004**, *50*, 9–16. [CrossRef]
7. Capelli, L.; Sironi, S.; Del Rosso, R.; Guillot, J.M. Measuring odours in the environment vs. dispersion modelling: A review. *Atmos. Environ.* **2013**, *79*, 731–743.
8. Han, Z.; Qi, F.; Li, R.; Wang, H.; Sun, D. Health impact of odour from on-situ sewage sludge aerobic composting throughout different seasons and during anaerobic digestion with hydrolysis pretreatment. *Chemosphere* **2020**, *249*, 126077. [CrossRef]
9. Henshaw, P.; Nicell, J.; Sikdar, A. Parameters for the assessment of odour impacts on communities. *Atmos. Environ.* **2006**, *40*, 1016–1029. [CrossRef]
10. Nicell, J.A. Assessment and regulation of odour impacts. *Atmos. Environ.* **2009**, *43*, 196–206. [CrossRef]
11. Schauberger, G.; Piringer, M.; Petz, E. Calculating direction-dependent separation distance by a dispersion model to avoid livestock odour annoyance. *Biosyst. Eng.* **2002**, *82*, 25–38. [CrossRef]
12. Piringer, M.; Knauder, W.; Petz, E.; Schauberger, G. Factors influencing separation distances against odour annoyance calculated by Gaussian and Lagrangian dispersion models. *Atmos. Environ.* **2016**, *140*, 69–83. [CrossRef]

13. Zhang, Q.; Zhou, X. Assessing Peak-to-Mean Ratios of Odour Intensity in the Atmosphere Near Swine Operations. *Atmosphere* **2020**, *11*, 224. [CrossRef]
14. Piringer, M.; Schauberger, G.; Petz, E.; Knauder, W. Comparison of two peak-to-mean approaches for use in odour dispersion models. *Water Sci. Technol.* **2012**, *66*, 1498–1501. [CrossRef]
15. Sykes, R.I.; Lewellen, W.; Parker, S.F. A Turbulent-Transport Model for Concentration Fluctuations and Fluxes. *J. Fluid Mech.* **1984**, *139*, 193–218. [CrossRef]
16. Bax, C.; Sironi, S.; Capelli, L. How Can odours Be Measured? An Overview of Methods and Their Applications. *Atmosphere* **2020**, *11*, 92. [CrossRef]
17. Riva, C.; Orzi, V.; Carozzi, M.; Acutis, M.; Boccasile, G.; Lonati, S.; Tambone, F.; D'Imporzano, G.; Adani, F. Short-term experiments in using digestate products as substitutes for mineral (N) fertilizer: Agronomic performance, odours, and ammonia emission impacts. *Sci. Total Environ.* **2016**, *547*, 206–214. [CrossRef]
18. Acutis, M.; Alfieri, L.; Giussani, A.; Provolo, G.; Guardo, A.D.; Colombini, S.; Bertoncini, G.; Castelnuovo, M.; Sali, G.; Moschini, M.; et al. ValorE: An integrated and GIS-based decision support system for livestock manure management in the Lombardy region (northern Italy). *Land Use Policy* **2014**, *41*, 149–162. [CrossRef]
19. *EN 13725:2003*; Air Quality-Determination of Odour Concentration by Dynamic Olfactometry. CEN: Brussels, Belgium, 2003.
20. Regione Lombardia. *Deliberazione Giunta Regionale 15 Febbraio 2012–n. IX/3018. Determinazioni Generali in Merito alla Caratterizzazione delle Emissioni Gassose in Atmosfera Derivanti da Attività a Forte Impatto Odourigeno. 2012, Boll. Uff. 20 Febbraio 2012 20–49*; Regione Lombardia: Milan, Italy, 2012.
21. Chowdhury, B.; Karamchandani, P.K.; Sykes, R.I.; Henn, D.S.; Knipping, E. Reactive puff model SCICHEM: Model enhancements and performance studies. *Atmos. Environ.* **2015**, *117*, 242–258. [CrossRef]
22. Karamchandani, P.; Vennam, P.; Shah, T.; Henn, D.; Alvarez-Gomez, A.; Yarwood, G.; Morris, R.; Brashers, B.; Knipping, E.; Kumar, N. Single source impacts on secondary pollutants using a Lagrangian reactive puff model: Comparison with photochemical grid models. *Atmos. Environ.* **2020**, *237*, 117664. [CrossRef]
23. Bradley, S.; Franco, M.; Hanna, S.H.; Howard, J.; Meris, R.; Mazzola, T.; Pate, B. Comparison of SCIPUFF predictions to SO_2 measurements from instruments on the MetOp-A, MetOp-B, Aura and Suomi satellites from the 2016 fire at Al-Mishraq. *Atmos. Environ.* **2021**, *245*, 118007. [CrossRef]
24. Deng, A.; Nelson, S.; Glenn, H.; David, S. Evaluation of interregional transport using the MM5-SCIPUFF system. *J. Appl. Meteorol.* **2004**, *43*, 1864–1886. [CrossRef]
25. Leelőssy, Á.; Molnár, F.; Izsák, F.; Havasi, Á.; Lagzi, I.; Mészáros, R. Dispersion modeling of air pollutants in the atmosphere: A review. *Open Geosci.* **2014**, *6*, 257–278. [CrossRef]
26. Onofrio, M.; Spataro., R.; Botta., S. A review on the use of air dispersion models for odour assessment. *Int. J. Environ. Pollut.* **2020**, *67*, 1–21. [CrossRef]
27. United States Environmental Protection Agency. *Guideline on Air Quality Models. Appendix W to Part 51. Federal Register, 2003, 68 (72), Tuesday, 15 April 2003/Rules and Regulations*; United States Environmental Protection Agency: Washington, DC, USA.
28. Bluett, J.; Gimson, N.; Fisher, G.; Heydenrych, C.; Freeman, T.; Godfrey, J. *Good Practice Guide for Atmospheric Dispersion Modelling*; Ministry for the Environment: Wellington, New Zealand, 2004.
29. MWLAP (Ministry of Water, Land & Air Protection, British Columbia). *Guidelines for Air Quality Dispersion Modelling in British Columbia*; British Columbia Ministry of Environment: Victoria, BC, Canada, 2003.
30. Sykes, R.I.; Parker, S.F.; Henn, D.S. Numerical simulation of ANATEX tracer data using a turbulent closure model for long-range dispersion. *J. Appl. Met.* **1993**, *32*, 929–947. [CrossRef]
31. Sykes, R.I.; Parker, S.F.; Henn, D.S.; Chowdhury, B. *SCIPUFF Version 3.2.2 Technical Documentation*; Sage Management: Princeton, NJ, USA, 2014; Volume 15, p. 393.
32. Holtslag, A.A.M.; van Ulden, A.P. A simple scheme for daytime estimates of the surface fluxes from routine weather data. *J. Clim. Appl. Met.* **1983**, *22*, 517–529. [CrossRef]
33. EPRI. *SCICHEM Version 3.2.2: Technical Documentation*; EPRI: Palo Alto, CA, USA, 2019.
34. Slade, D.H. *Meteorology and Atomic Energy*; U.S. Atomic Energy Commission, Office of Information Services: Germantown, MD, USA, 1968; 445p.
35. Lewellen, W.S. *Use of invariant modeling. Handbook of Turbulence*; Frost, W., Moulden, T.H., Eds.; Plenum Press: New York, NY, USA, 1977; pp. 237–280.
36. Lewellen, W.S.; Sykes, R.I. Analysis of concentration fluctuations from lidar observations of atmospheric plumes. *J. Clim. Appl. Met.* **1986**, *25*, 1145–1154.
37. Yee, E. The shape of the probability density function of short-term concentration fluctuations of plumes in the atmospheric boundary layer. *Bound. Layer Meteorol.* **1990**, *51*, 269–298. [CrossRef]
38. Schulman, L.L.; Strimaitis, D.G.; Scire, J.S. Addendum to ISC3 User's Guide: The PRIME Plume Rise and Building Downwash Model. 1997. Available online: https://gaftp.epa.gov/aqmg/SCRAM/models/other/iscprime/useguide.pdf (accessed on 15 August 2022).
39. Schulman, L.L.; Strimaitis, D.G.; Scire, J.S. Development and Evaluation of the PRIME Plume Rise and Building Downwash Model. *J. Air Waste Manag. Assoc.* **2000**, *50*, 378–390. [CrossRef]

40. De Melo Lisboa, H.; Guillot, J.M.; Fanlo, J.L.; Le Cloirec, P. Dispersion of odourous gases in the atmosphere—Part I: Modeling approaches to the phenomenon. *Sci Total Environ.* **2006**, *361*, 220–228. [CrossRef]
41. Ucar, T.; Hall, F.R. Windbreaks as a pesticide drift mitigation strategy: A review. *Pest Manag. Sci.* **2001**, *57*, 663–675. [CrossRef]
42. Williams, M.L.; Thompson, N. The effects of weather on odour dispersion from livestock buildings and from fields. In *Odour Prevention and Control or Organic Sludge and Livestock Farming*; Nielsen, V.C., Voorburg, J.H., L'Hermite, P., Eds.; Elsevier: New York, NY, USA, 1985; pp. 227–233.
43. Guo, H.; Jacobson, L.D.; Schmidt, D.R.; Nicolai, R.E. Evaluation of the influence of atmospheric conditions on odour dispersion from animal production sites. *Trans. ASAE* **2003**, *46*, 461. [CrossRef]
44. Canepa, E. An overview about the study of downwash effects on dispersion of airborne pollutants. *Environ. Model. Softw.* **2004**, *19*, 1077–1087. [CrossRef]
45. Jeanjean, A.P.R.; Monks, P.S.; Leigh, R.J. Modelling the effectiveness of urban trees and grass on PM2.5 reduction via dispersion and deposition at a city scale. *Atmos. Environ.* **2016**, *147*, 1–10. [CrossRef]
46. Tong, Z.; Baldauf, R.W.; Isakov, V.; Deshmukh, P.; Max Zhang, K. Roadside vegetation barrier designs to mitigate near-road air pollution impacts. *Sci. Total Environ.* **2016**, *541*, 920–927. [CrossRef]
47. O'Neill, D.H.; Phillips, V.R. A review of the control of odour nuisance from livestock buildings: Part 3, properties of the odorous substances which have been identified in livestock wastes or in the air around them. *J. Agric. Eng. Res.* **1992**, *53*, 23–50. [CrossRef]
48. Tzilivakis, J.; Lewis, K.; Green, A.; Warner, D. *The Climate Change Mitigation Potential of an EU Farm: Towards a Farm-Based Integrated Assessment*; ENV.B.1/ETU/2009/0052, Final Report; University of Hertfordshire: Hertfordshire, UK, 2010.
49. Gifford, F. Statistical Properties of A Fluctuating Plume Dispersion Model. In *Advances in Geophysics*; Landsberg, H.E., Van Mieghem, J., Eds.; Elsevier: Amsterdam, The Netherlands, 1959; pp. 117–137.
50. de Bree, F.; Harssema, H. Field Evaluation of a Fluctuating Plume Model for Odours with Sniffing Teams. In *Environmental Meteorology: Proceedings of an International Symposium Held in Würzburg, F.R.G., Würzburg, Germany, 29 September–1 October 1987*; Grefen, K., Löbel, J., Eds.; Springer: Dordrecht, The Netherlands, 1988; pp. 473–486. [CrossRef]
51. Dourado, H.; Santos, J.M.; Reis, N.C.; Mavroidis, I. Development of a fluctuating plume model for odour dispersion around buildings. *Atmos. Environ.* **2014**, *89*, 148–157. [CrossRef]
52. Mussio, P.; Gnyp, A.; Henshaw, P. A fluctuating plume dispersion model for the prediction of odour-impact frequencies from continuous stationary sources. *Atmos. Environ.* **2001**, *35*, 2955–2962. [CrossRef]
53. Belgiorno, V.; Naddeo, V.; Zarra, T. *Odour Impact Assessment Handbook*; John Wiley & Sons: Hoboken, NJ, USA, 2012.
54. Högström, U. A method for predicting odour frequencies from a point source. *Atmos. Environ.* **1972**, *6*, 103–121. [CrossRef]
55. Nordic Council of Ministers, N. *Abatement Control and Regulation of Emission and Ambient Concentration of Odour and Allergens from Livestock Farming*; Nordiska Ministerrådets Förlag: Copenhagen, Denmark, 2009.
56. PSU; PDA. *Odor Management in Pennsylvania A Reference Manual*; Robin, C.B., Herschel, A.E., Eds.; Penn State University: State College, PA, USA; PDA: Bethesda, MA, USA, 2002.
57. United Kingdom Environmental Agency. *Integrated Pollution Prevention and Control (IPPC). Horizontal Guidance for Odour Part 1–Regulation and Permitting*; United Kingdom Environmental Agency: Bristol, UK, 2002.
58. Cimorelli, A.; Perry, S.; Venkatram, A.; Weil, J.; Paine, R.; Wilson, R.; Lee, R.; Peters, W.; Brode, R. AERMOD: A dispersion model for industrial source applications. Part I: General model formulation and boundary layer characterization. *J. Appl. Meteorol.* **2005**, *44*, 682–693. [CrossRef]
59. Stocker, J.; Ellis, A.; Smith, S.; Carruthers, D.; Venkatram, A.; Dale, W.; Attree, M. A review of dispersion modelling of agricultural emissions with non-point sources. *Int. J. Environ. Pollut.* **2017**, *62*, 247–263. [CrossRef]
60. Vieira de Melo, A.M.; Santos, J.M.; Mavroidis, I.; Reis Junior, N.C. Modelling of odour dispersion around a pig farm building complex using AERMOD and CALPUFF. Comparison with wind tunnel results. *Build. Environ.* **2012**, *56*, 8–20. [CrossRef]
61. EPA. *Guideline on Air Quality Models, Appendix W to 40 CFR*; Part 51; United States Environmental Protection Agency: Washington, DC, USA, 2017.
62. Carruthers, D.; Kala, A. Odour Modelling Using ADMS Software. CERC-ELLE Presentation. 2012. Available online: http://gamta.lt/files/Aiga%20Kala%20ELLE-ADMS%20odour%2020120202.pdf (accessed on 13 February 2022).
63. Loubet, B.; Genermont, S.; Ferrara, R.; Bedos, G.; Decuq, G.; Personne, E.; Fanucci, O.; Durand, B.; Rana, G.; Cellier, P. An inverse model to estimate ammonia emissions from fields. *Eur. J. SOIL Sci.* **2010**, *61*, 793–805. [CrossRef]
64. Loubet, B.; Milford, C.; Sutton, M.A.; Cellier, P. Investigation of the interaction between sources and sinks of atmospheric ammonia in an upland landscape using a simplified dispersion-exchange model. *J. Geophys. Res. Atmos.* **2001**, *106*, 24183–24195. [CrossRef]
65. Bedos, C.; Loubet, B.; Barriuso, E. Gaseous Deposition Contributes to the Contamination of Surface Waters by Pesticides Close to Treated Fields. A Process-Based Model Study. *Environ. Sci. Technol.* **2013**, *47*, 14250–14257. [CrossRef]
66. Huang, C.H. A theory of dispersion in turbulent shear flow. *Atmos. Environ.* **1979**, *13*, 453–463. [CrossRef]
67. Danuso, F.; Rocca, A.; Ceccon, P.; Ginaldi, F. A software application for mapping livestock waste odour dispersion. *Environ. Model. Softw.* **2015**, *69*, 175–186. [CrossRef]
68. Hanna, S.R.; Briggs, G.A.; Hosker, J.R.P. *Handbook on Atmospheric Diffusion*; National Oceanic and Atmospheric Administration: Oak Ridge, TN, USA, 1982. [CrossRef]

69. Cirillo, M.C.; Poli, A.A. An intercomparison of semiempirical diffusion models under low wind speed, stable conditions. *Atmos. Environ. Part Gen. Top.* **1992**, *26*, 765–774. [CrossRef]
70. Provincia di Rovigo. *Valutazione di Compatibilità Ambientale e Contestuale Rilascio Dell'autorizzazione Integrata Ambientale per Ampliamento di un Allevamento Avicolo a Taglio di Po (RO)-Denominato PO3. 2015, Bur n. 36 del 10 Aprile 2015*; Provincia di Rovigo: Rovigo, Italy.
71. Rodean, H.C. *Notes on the Langcvin Modcl for Turbulent Diffusion of "Marked" Particles*; UCRL-ID-115869 Report; Lawrence Livermore National Laboratory: Livermore, CA, USA, 1994.
72. Wilson, J.D.; Sawford, B.L. Review of Lagrangian stochastic models for trajectories in the turbulent atmosphere. *Bound. -Layer Meteorol.* **1996**, *78*, 191–210. [CrossRef]
73. Flesch, T.K.; Wilson, J.D.; Harper, L.A. Deducing Ground-to-Air Emissions from Observed Trace Gas Concentrations: A Field Trial with Wind Disturbance. *J. Appl. Meteorol.* **2005**, *44*, 475–484. [CrossRef]
74. Flesch, T.K.; Wilson, J.D.; Harper, L.A.; Crenna, B.P.; Sharpe, R.R. Deducing Ground-to-Air Emissions from Observed Trace Gas Concentrations: A Field Trial. *J. Appl. Meteorol.* **2004**, *43*, 487–502. [CrossRef]
75. Vesenmaier, A.; Reiser, M.; Zarra, T.; Naddeo, V.; Belgiorno, V.; Kranert, M. Fugitive Methane and Odour Emission Characterization at a Composting Plant using Remote Sensing Measurements. *Glob. Nest J.* **2018**, *20*, 674–677.
76. Zhou, X.J.; Zhang, Q.; Guo, H.; Li, Y.X. Evaluation of Air Dispersion Models for Livestock Odour Application. In Proceedings of the CSAE/SCGR 2005 Meeting, Winnipeg, Manitoba, 26–29 June 2005.
77. Tinarelli, G.; Giostra, U.; Ferrero, E.; Tampieri, F.; Anfossi, D.; Brusasca, G.; Trombetti, F. SPRAY, A 3-D Particle Model for Complex Terrain Dispersion. In Proceedings of the 10th Symposium on Turbulence and Diffusion, American Meteorological Society, Portland, OR, USA, 29 September–2 October 1992; pp. 147–150.
78. Tinarelli, G.; Anfossi, D.; Bider, M.; Ferrero, E.; Trini Castelli, S. A new high performance version of the Lagrangian particle dispersion model SPRAY, some case studies. In *Air Pollution Modelling and its Application XIII*; Gryning, S.E., Batchvarova, E., Eds.; Plenum Press: New York, NY, USA, 2000; Volume 23, pp. 499–506. ISBN 0-306-46188-9.
79. Tinarelli GSozzi, R.; Trini Castelli, S.; Bisignano, A. *Inserimento e Verifica di Algoritmi per il Calcolo del Peak-to-Mean Ratio in un Modello a Particelle*; Oral Presentation, festival ECOMONDO; ECOMONDO: Rimini, Italy, 2019.
80. Schauberger, G.; Piringer, M.; Petz, E. Steady-state balance model to calculate the indoor climate of livestock buildings, demonstrated for finishing pigs. *Int. J. Biometeorol.* **2000**, *43*, 154–162. [CrossRef]
81. Mylne, K.R.; Mason, P.J. Concentration fluctuation measurements in a dispersing plume at a range of up to 1000 m. *Q. J. R. Meteorol. Soc.* **1991**, *117*, 177–206. [CrossRef]
82. Mylne, K.R. Concentration fluctuation measurements in a plume dispersing in a stable surface layer. *Bound.-Layer Meteorol.* **1992**, *60*, 15–48. [CrossRef]
83. Brusasca, G.; Carboni, G.; Finardi, S.; Sanavio, D.; Tinarelli, G.; Toppetti, A. Comparison of a Gaussian (ISC3) and a Lagrangian Particle Model (SPRAY) for Regulatory applications in Flat and Complex Terrain Sites Representative of Typical Italian Landscape. In Proceedings of the 7th International Conference on Harmonization within Atmospheric Dispersion Modelling for Regulatory Purposes, Belgirate, Italy, 28–31 May 2001.
84. Gariazzo, C.; Papaleo, V.; Pelliccioni, A.; Calori, G.; Radice, P.; Tinarelli, G. Application of a Lagrangian particle model to assess the impact of harbour, industrial and urban activities on air quality in the Taranto area, Italy. *Atmos. Environ. Harb. Air Qual.* **2007**, *41*, 6432–6444. [CrossRef]
85. Stohl, A.; Forster, C.; Frank, A.; Seibert, P.; Wotawa, G. Technical note: The Lagrangian particle dispersion model FLEXPART version 6.2. *Atmos. Chem. Phy.* **2005**, *5*, 2461–2474. [CrossRef]
86. Luhar, A.K.; Hibberd, M.F.; Hurley, P.J. Comparison of closures schemes used to specify the velocity PDF in Lagrangian stochastic dispersion models for convective conditions. *Atmos. Environ.* **1996**, *30*, 1407–1418. [CrossRef]
87. Emanuel, K.A. A scheme for representing cumulus convection in large-scale models. *J. Atmos. Sci.* **1991**, *48*, 2313–2335. [CrossRef]
88. Safi, K.; Gagliardo, A.; Wikelski, M.; Kranstauber, B. How Displaced Migratory Birds Could Use Volatile Atmospheric Compounds to Find Their Migratory Corridor: A Test Using a Particle Dispersion Model. *Front. Behav. Neurosci.* **2016**, *10*, 175. [CrossRef]
89. Draxler, R.R.; Hess, G.D. *Description of the HYSPLIT_4 Modeling System*; NOAA Technical Memorandum, ERL ARL-224; NOAA Air Resources Laboratory: Silver Spring, MD, USA, 1997; 24p.
90. Teixeira, S.; Pereira, P.; Ferreira, F. Atmospheric Odours: Monitoring of an Urban Waste Operator with Citizen Participation. *Chem. Eng. Trans.* **2018**, *68*, 91–96.
91. Wacuka, C.; Muthama, N.; Ng'ang'a, J.; Mutai, B. Simulation of odour Transport and Dispersion from a Waste Water Treatment Plant: A case study of Kahawa Ward Nairobi County. *J. Clim. Chang. Sustain.* **2016**, *1*, 58–68. [CrossRef]
92. Cao, X.; Roy, G.; Hurley, W.J.; Andrews, W.S. Dispersion Coefficients for Gaussian Puff Models. *Bound. Layer Meteorol.* **2011**, *139*, 487–500. [CrossRef]
93. DeVito, T.J.; Cao, X.; Roy, G.; Costa, J.R.; Andrews, W.S. Modelling aerosol concentration distributions from transient (puff) sources. *J. Environ. Eng. Sci.* **2013**, *8*, 255–266. [CrossRef]
94. Scire, J.S.; Insley, E.M.; Yamartino, R.J. *Model Formulation and User's Guide for the CALMET Meteorological Model*; California Air Resources Board by Sigma Research Corporation: Concord, MA, USA, 1990.
95. Abdul-Wahab, S.; Sappurd, A.; Al-Damkhi, A. Application of California Puff (CALPUFF) model: A case study for Oman. *Clean Technol. Environ. Policy* **2011**, *13*, 177–189. [CrossRef]

96. Capelli, L.; Sironi, S.; Del Rosso, R.; Céntola, P.; Rossi, A.; Austeri, C. Olfactometric approach for the evaluation of citizens' exposure to industrial emissions in the city of Terni, Italy. *Sci. Total Environ.* **2011**, *409*, 595–603. [CrossRef]
97. Çetin Doğruparmak, Ş.; Pekey, H.; Arslanbaş, D. Odour dispersion modeling with CALPUFF: Case study of a waste and residue treatment incineration and utilization plant in Kocaeli, Turkey. *Environ. Forensics* **2018**, *19*, 79–86. [CrossRef]
98. Busini, V.; Capelli, L.; Sironi, S.; Nano, G.; Rossi, A.; Bonati, S. Comparison of CALPUFF and AERMOD Models for Odour Dispersion Simulation. *Chem. Eng. Trans.* **2012**, *30*, 205–210. [CrossRef]
99. Wang-Li, L.; Parker, D.; Parnell, C.; Lacey, R.; Shaw, B. Comparison of CALPUFF and ISCST3 models for predicting downwind odour and source emission rates. *Atmos. Environ.* **2006**, *40*, 4663–4669. [CrossRef]
100. Sykes, R.I.; Parker, S.F.; Henn, D.S.; Gabruk, R.S. SCIPUFF—A Generalized Dispersion Model. In *Air Pollution Modeling and Its Application XI, NATO—Challenges of Modern Society*; Gryning, S.-E., Schiermeier, F.A., Eds.; Springer: Boston, MA, USA, 1996; pp. 425–432. [CrossRef]
101. Porter, R. Peak-to-Mean Ratios for odour Impacts: A Tracer Study Revisited. *Proc. Water Environ. Fed.* **2006**, *2006*, 63–78. [CrossRef]
102. Yamartino, R.J.; Scire, J.S.; Carmichael, G.R.; Chang, Y.S. The CALGRID mesoscale photochemical grid model—I. Model formulation. *Atmos. Environ. Part Gen. Top.* **1992**, *26*, 1493–1512. [CrossRef]